FINDING FLYBYS IN THE ILLUSTRIS SIMULATION

By

Christina Davis

Dissertation

Submitted to the Faculty of the

Graduate School of Vanderbilt University

in partial fulfillment of the requirements

for the degree of

DOCTOR OF PHILOSOPHY

in

Astrophysics

August 31, 2021

Nashville, Tennessee

Approved:

Kelly Holley-Bockelmann, Ph.D.

Andreas Berlind, Ph.D.

Manodeep Sinha, Ph.D.

David Weintraub, Ph.D.

Dedication

I dedicate this thesis to

My Parents,

For supporting me wholeheartedly no matter where my curiosity took me,

and

Nick

For never letting me forget what's possible,

and working alongside me every step of the way.

Acknowledgment

An endless thank you to Dr. Kelly Holley-Bockelmann for sticking with me throughout the years, and building me into a more capable and confident scientist. She has helped me over more hurdles than I can count, and none of this would have been possible without her creative solutions, endless encouragement, and expert advice.

I'm grateful for my extended research family including my committee members Dr. David Weintraub, Dr. Andreas Berlind, and Dr. Manodeep Sinha, as well as the members of the multi-generational X-Gal research group. I thank Dr. Bill Gabella for his endless kindness and sustained willingness to help.

Thank you to my friends Dr. Kyle Conroy, Dr. Meagan Lang, Gabriella Elan Alvarez Clapper, Nicole Sanchez, and Anna Egnar for being the family that is there to celebrate every accomplishment, commiserate every setback, and brainstorm every solution.

A huge thanks to Kelsey Anderson and the Anderson family for keeping things in perspective and giving me a place to study from high school all the way to writing these last few sections.

I thank my parents for always encouraging me to follow my interests and prioritizing my education throughout my life. Their enthusiasm and support has been invaluable.

Finally, I thank Nick Chason who has pushed me to develop my own scientific curiosity, believed in me continuously, and been a true teammate through each phase of this journey.

TABLE OF CONTENTS

LIST OF TABLES

LIST OF FIGURES

Chapter 1

Introduction

Galaxies in the Universe are not static objects, but are constantly evolving massive structures made of dark matter, stars, and gas. Galaxies are formed inside large clouds of dark matter, which account for the vast majority of mass. All of these components engage together to give a galaxy its overall appearance in shape, color, mass, and activity. For decades, galaxy interactions in the form of mergers have been credited as the key motivator of galaxy evolution. Mergers are common throughout the universe, their rates and effects have been studied extensively over the years, but there exists a separate type of dynamical interaction that has the capacity to alter a galaxy – flybys. A galaxy flyby occurs when the dark matter halos of two independent galaxies interpenetrate and later detach. The perturbations induced by flybys can generate long lasting changes both in the intruder and the victim (Lang et al., 2014).

As galaxy-galaxy interactions may take place over billions of years, an invaluable way to study these interactions is via N-body simulations. Using cosmological, hydrodynamical simulations we are able to observe a large sample of halos interact naturally throughout the universe. In this thesis I explore the commonality and dynamical characteristics of flybys in a cosmological context by analyzing the Illustris Simulation (Nelson et al., 2015).

1.1 Current Cosmological Perspective

In order to fully appreciate the intricacies of galaxy evolution and the validity of simulations to uncover such truths, we must first set the cosmological stage. The beginning of the universe as we know it, started with all existing matter packed densely into a near-infinitely small volume and rapidly expanding in an event we call the Big Bang. At that time, the universe was hot, dense and nearly isotropic in form, and overall looked and behaved extremely differently from what we observe today. However, during the infancy of the universe, quantum fluctuations created minor temperature differences which planted

the seeds for what would become the dominant structures in the universe today, 13.7 billion years later.

The prediction of such an event was verified midway through the 20th century with detections of the Cosmic Microwave Background (CMB) (Penzias & Wilson, 1965; Sachs & Wolfe, 1967). The light detected in the CMB are the first photons able to travel unimpeded through the cosmos, and have stretched with space itself along the way. By studying the CMB, astronomers have been able to unlock many invisible characteristics that have played a role in shaping our universe and combine these concepts into a self-consistent cosmic perspective that appropriately fits the wide variety of observations made, which we call ΛCDM.

The ΛCDM model describes key cosmological traits of our universe, and divides the matter-energy content into three primary categories: dark energy, dark matter, and baryonic matter. The first is represented by Λ, the cosmological constant, which characterizes the dark energy content of the Universe. Dark energy is an elusive energy type, but is crucially responsible for the expansion of the Universe. While the specific characteristics of dark energy remain a mystery, the rate of expansion of the universe is well-characterized and can be reliably modeled using analytic equations as well as simulations. Second, CDM stands for cold dark matter, which astronomers believe to make up 85% of the matter in the universe (Ade et al., 2016). The word "cold" describes the non-relativistic nature, implying it moves slowly compared to the speed of light. The "dark" quality is what fundamentally separates it from other types of matter. Dark matter does not emit electromagnetic radiation, and interacts only weakly with light through its gravitational field. This leaves all other known types of matter as the third category of matter, which we call baryonic matter. Baryonic matter includes all luminous matter such as stars, gas, and what we would consider "normal matter."

1.1.1 Physics of Dark Matter

Dark matter is central to the concept of galaxy evolution as it is the dominate component of mass and therefore dominates the gravitational effects on large scales. But why do astronomers find the need to invoke this type of invisible matter at all in their models? Dark matter's existence was put forth as a far-fetched theory by early 20th century astronomer Fritz Zwicky to explain high speeds of galaxies within galaxy clusters (Zwicky, 1937). The estimated mass from luminous sources was not nearly enough to account for high speeds measured for cluster galaxies, so there must be a large sum of unaccounted for invisible mass.

At the time, the concept of dark matter was not well-received, and there were numerous errors with Zwicky's measurements. It wasn't until 1970 when strong empirical evidence for dark matter began to gain traction. Vera Rubin measured rotational velocities, v_{rot}, of stars and globular clusters far outside the visible extent of a galaxy (Rubin & Ford, 1970). If the mass of the galaxy was limited to the luminous portion, we'd expect the velocities of far away stellar objects to drop at an expected rate of $v_{rot} \propto 1/r^2$. Instead, Rubin found that the rotational velocities remained constant out to much farther distances than the bright component of the galaxy could account for. What astronomers came to realize was that this was not just true for some particular galaxies, but nearly every observable galaxy was surrounded with an expansive and massive fog of dark matter (Rubin et al., 1980).

We now call this massive haze enveloping galaxies, the *dark matter halo*. In the case of our own Milky Way galaxy, the stellar component has a mass of $6 \times 10^{10} M_{\odot}$ and the stellar disk spans a diameter of roughly 30 kpc, but the dark matter halo has a mass closer to $10^{12} M_{\odot}$ and stretches nearly 500 kpc across (Licquia & Newman, 2015). Throughout the universe, dark matter is the invisible building block, dominated by gravitational forces, it clumps and merges and dictates much of the behavior of the visible parts of the galaxies we observe.

Dark matter halos are constructed via a process called hierarchical structure formation,

which simply tells us that small halos are formed first and then merge with other halos to build up mass into the large structures that we see today. As dark matter's behavior is dictated by gravitational forces, the initial points of overdensity set in the early stages of the universe are the first locations that start collecting mass, and house today some of the largest galaxies and galaxy clusters in existence.

1.2 Galaxy Evolution

Galaxies themselves are composed of much more than dark matter, they are made of gas, stars, dust, black holes, and much more. But how these objects manifest and the overall shapes, sizes, and colors of galaxies are very dependent on the halo's assembly and history. Smooth accretion, or the slow and gentle accumulation of mass, is only one avenue of galaxy evolution, but interactions have proven to be extremely transformative.

For decades, astronomers have observed close pairs of galaxies and noted that distorted features such as tails or rings could be the result of merging galaxies (Zwicky, 1956, 1959). Studying galaxy interactions, which happen on the scale of Gyrs is extremely tough to do using only observational tools. With the ever-increasing sophistication of computer simulations, we have been able to verify that interactions are capable of dramatically changing the appearance and contents of galaxies (Dubinski & Chakrabarty, 2009).

Tidal forces between two merging galaxies were shown to be able to string out long tidal tails or rings of gas and stars (Toomre & Toomre, 1972; White, 1979; Naab & Burkert, 2003; Lynds & Toomre, 1976). These changes in morphology depend on a variety of parameters including mass ratio between the halos, their relative sizes and proximity, and orbital parameters including whether the interaction is prograde or retrograde (Hernquist & Weinberg, 1989). In the case of a galaxy interacting with another several orders of magnitude larger, the larger galaxy may resist any changes brought on by the encounter, and it's possible the smaller could be completely destroyed or consumed (Hernquist & Weinberg, 1989; Weinberg, 1998; Holley-Bockelmann & Richstone, 2000).

Tidal forces from an encounter can do more to a galaxy than change the morphology, they can also compress gas and create overdense regions which become ripe for star formation. These star forming bursts have been seen in both observations (van der Hulst, 1979; Whitaker et al., 2014) and simulations (Mihos & Hernquist, 1996; Naab & Burkert, 2003).

Interactions, including flybys, have also been shown to induce bars in galaxies, which themselves can induce further changes to the contents of a galaxy (Lang et al., 2014). Simulations revealed that cold disks of galaxies are kinematically unstable and will form bars when perturbed (Toomre, 1964; Dubinski & Chakrabarty, 2009). Predictions from linear perturbation theory and N-body simulations reveal that bars formed due to interactions from other galaxies may grow to be larger than their isolated counterparts (Holley-Bockelmann et al., 2005; Weinberg & Katz, 2002).

Bars themselves can be long-lived features that are visible for several Gyrs after an encounter (Lang et al., 2014). They also have the power to transform the galaxy in their own right by funneling gas from the outskirts to the central regions of the galaxy. This could result in a star formation episode, or the fueling of a central black hole and creation of an active galactic nuclei (AGN) (Shlosman et al., 1989; Hopkins & Quataert, 2010).

Simulations of feedback regulated black holes show that interactions themselves are also able to fuel AGN by forcing gas inwards. These simulations have been able to accuracy reproduce known relations between galaxies and their black holes including $M_b - M_{BH}$ and $M_{BH} - \sigma_b$, the mass of a black hole and the galaxy's velocity dispersion, σ_b, indicating that these processes are consistent with observational properties of galaxies (Di Matteo et al., 2005; Tremaine et al., 2002; Marconi & Hunt, 2003).

Overall, interactions and primarily mergers, have proven to be effective as motivating change in galaxies. Mergers are extremely common in the universe and are one of the fundamental drivers of galaxy evolution and growth (Lacey & Cole, 1993). We have shown that flybys have the potential to be transformative to galaxies, but few researches incorporate a search for flybys when calculating interaction rates.

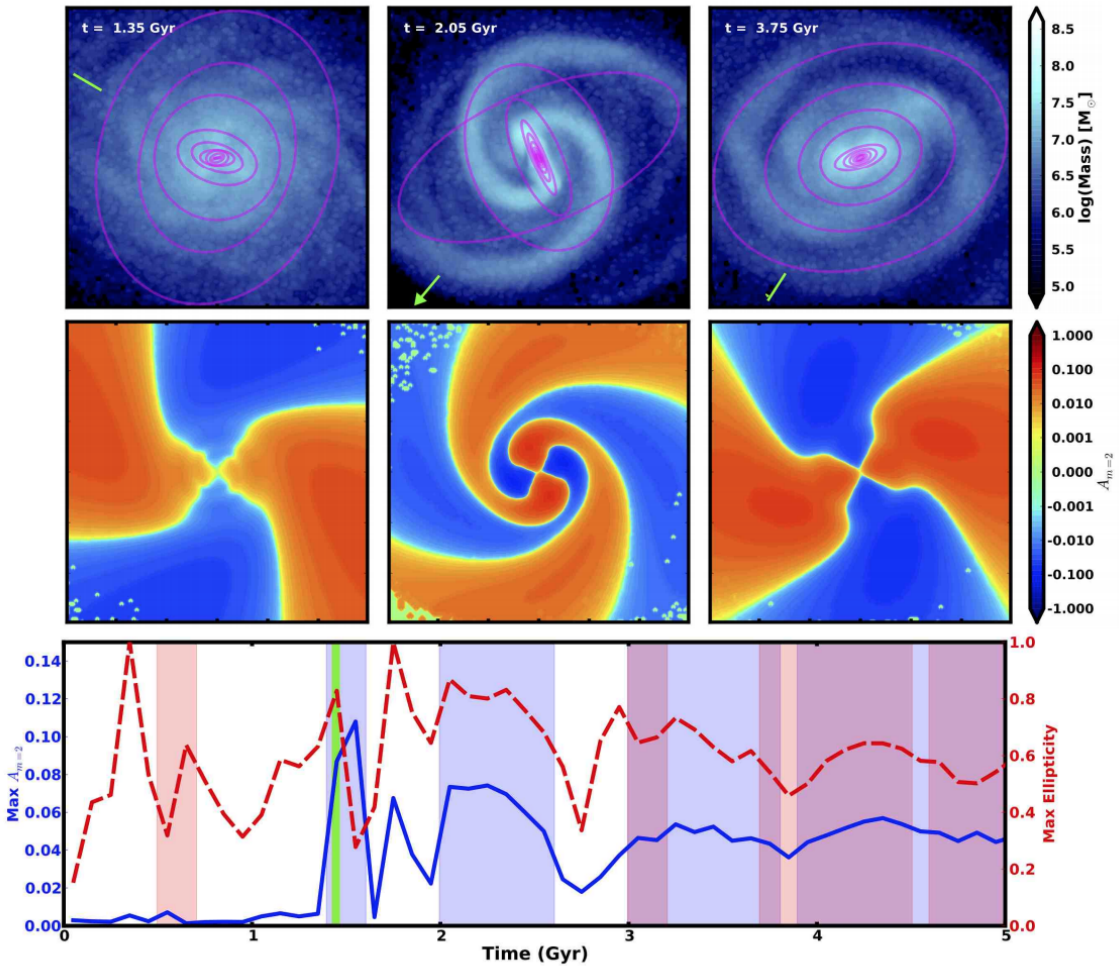

Figure 1.1: Measured effects from a 1:1 Prograde Flyby Simulation as seen in Lang et al. (2014). Top panel shows projected mass distributions of the inner 30 kpc fitted with magenta ellipses. Middle panel shows the amplitude of the $m = 2$ mode which corresponds to a bar. Bottom panel shows the full time evolution of $A_{m=2}$ where the green vertical line marks the pericenter of the interaction. Shaded regions indicate where bar criteria is met, blue and red correspond to SCF and ellipse fitting respectively. Flybys are successfully able to create long-lasting mergers in isolated simulations.

1.3 Cosmological Simulations

Simulations of dark matter halos and galaxies have become invaluable to understanding how the universe came to look the way it does today. Cosmological timescales present challenges to observational studies of the evolution of galaxies and large scale structure. By pairing what we observe at different times in the universe with simulations of what we believe to be the main physics at play, has given us a powerful tool to unlock many mysteries of galaxy formation.

In principle, simulations work by setting test particles in a volume and allowing their movement on fixed timescales to be determined by gravity. As we know that the majority of mass in the universe is dark matter, which although mysterious in nature, behaves in a very predictable way. The difficulty comes with the computational cost of directly computing forces between all test particles. For N test particles, to directly compute the force on each particle requires N^2 operations at each evolved timestep. Early simulations used as few as 250 test particles placed in a simple gravitational potential (White, 1978; Holmberg, 1941). But the proof of the utility in simulations was evident as we were able to reproduce observed structures of galaxies including bars and tidal tails (D'Onghia et al., 2010; Barnes, 1988; Springel & White, 1999).

Since then, simulations have increased significantly in sophistication. The N^2 process of directly computing the gravitational force between all particles in a box becomes too costly when trying to simulate a cosmological volume with a large dynamic range. Instead, the forces of distant particles are cleverly estimated based on low order multipole expansions which reduces the order of computations to NlogN. This allowed for a massive increase in the number of particles used and thus higher resolution simulations.

Resolution of simulations is tailored to the needs of the object of interest. For some, studying individual galaxies and their internal structure means using isolated or "zoom-in" simulations. Similarly, an interest in the demographics of how galaxies interact on a large scale across cosmic time lends itself to the use of cosmological simulations. Cosmological

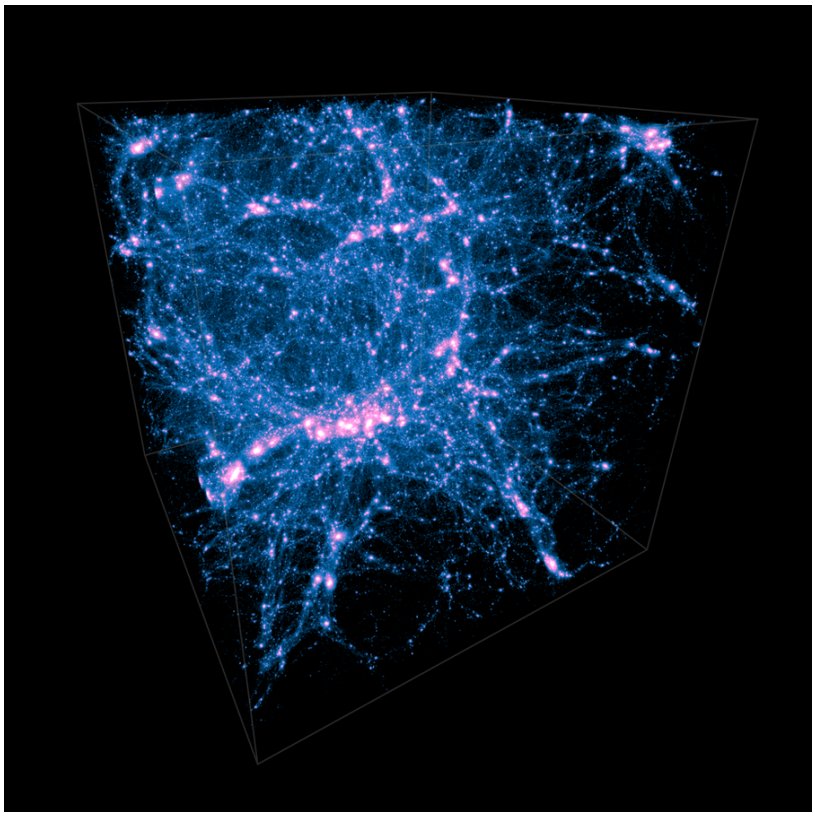

Figure 1.2: An exterior view of the dark matter density in the Illustris-1 simulation. Each side of the simulation box is 106.5 Mpc. Bright pink areas show high density knots at the intersection of large filaments of dark matter. Galaxies and galaxy clusters reside in the dense centers of these dark matter structures. Image from the Illustris Collaboration, 2018 (https://www.illustris-project.org/).

simulations span Mpcs to Gpcs of space as to encompass not only the galaxy of interest, but its local neighborhood. These types of simulations are able to capture a broad picture of galaxy growth as it interacts and accumulates mass from nearby structures. The resolution of a given simulation is set by the "softening length" between particles, which describes the point at which the positions and forces of the particles are unreliable. This springs from the fact that as massive objects are attracted by gravity, their gravitational force continues to increase. When two particles approach each other at distances below the softening length, the force between them increases unrealistically, and thus we artificially "soften" the force between them (Bertschinger, 1998).

1.3.1 Dark Matter Only versus Hydrodynamic Runs

Dark matter only simulations (DMO) simply capture the gravitational effects of dark matter and the locations of galaxies are inferred after the fact and then compared to observations. The convenience of dark matter is that gravitational effects are extremely well known, however in the connection to observations, there are many parameters left to tune to accurately place galaxies in their corresponding halos (Berlind et al., 2003). A second category of simulations are hydrodynamic simulations which attempt to model physics of baryonic matter as well in the form of star formation, gas physics, black hole feedback, and more. Hydrodynamic (hydro) simulations rely on tuning these prescriptions to observations and aim to combine the net effects of multiple kinds of forces on a galaxy (Vogelsberger et al., 2013). The benefit to hydro simulations is the ease of comparison with observation, but this comes at the cost of adding complication to the physics models and computational expense.

Many groups have investigated the differences in DMO and hydro simulations and found that while baryonic matter makes up only a small fraction of the total mass in a galaxy, their effects can have profound implications on galaxy dynamics. Incorporating energy output from supernova as well as black hole feedback in the form of AGN, pushes gas

outwards and can affect the stellar distribution as well as the overall potential of a galaxy (El-Badry et al., 2016). Several side-by-side investigations between hydro and DMO simulations have found a suppressive effect on halo formation leading to slightly lower masses, fewer subhalos, and less dense halos (Zolotov et al., 2012; Brooks et al., 2013; Brooks & Zolotov, 2014; Chua et al., 2017; Beltz-Mohrmann & Berlind, 2021).

In this thesis we will create interaction networks including mergers and flybys for three hydrodynamic realizations of the Illustris simulation at varying resolution and one accompanying DMO version (Illustris-3 Dark). We measure the effects that the addition of baryonic physics has on merger and flyby rates for halos across time.

1.3.2 The Illustris Simulation

The Illustris simulation is a high-resolution suite of hydrodynamical simulations of a $(106.5\text{Mpc})^3$ volume. The simulation starts at $z = 127$ and evolves to present day ($z = 0$), providing 13.7 billion years of evolution with high temporal cadence (Nelson et al., 2015). With 135 snapshots and three levels of resolution using up to $(1820)^3$ particles, the Illustris simulation is ideal for studying flybys and their many physical properties. The Illustris simulation includes the physics of star formation, feedback, and evolution, super- massive black hole growth, AGN and supernova feedback, and gas cooling. It also has a large dynamic range of masses and includes over 10^3 Milky Way-like halos. This allows us to observe the effects of flybys on a large variety of galaxy types and histories.

Figure 1.2 shows an exterior view of the Illustris volume. The image shows the dark matter distribution across the box with bright pink areas showing extremely dense areas of dark matter which are likely to host galaxy clusters be the site of frequent interactions. The Illustris simulation has successfully reproduced many well-known observational relationships such as cosmic star formation rate density, galaxy luminosity functions, and galaxies obey the stellar and baryonic Tully-Fisher relation (Rodriguez-Gomez et al., 2015; Vogelsberger et al., 2014; Genel et al., 2014).

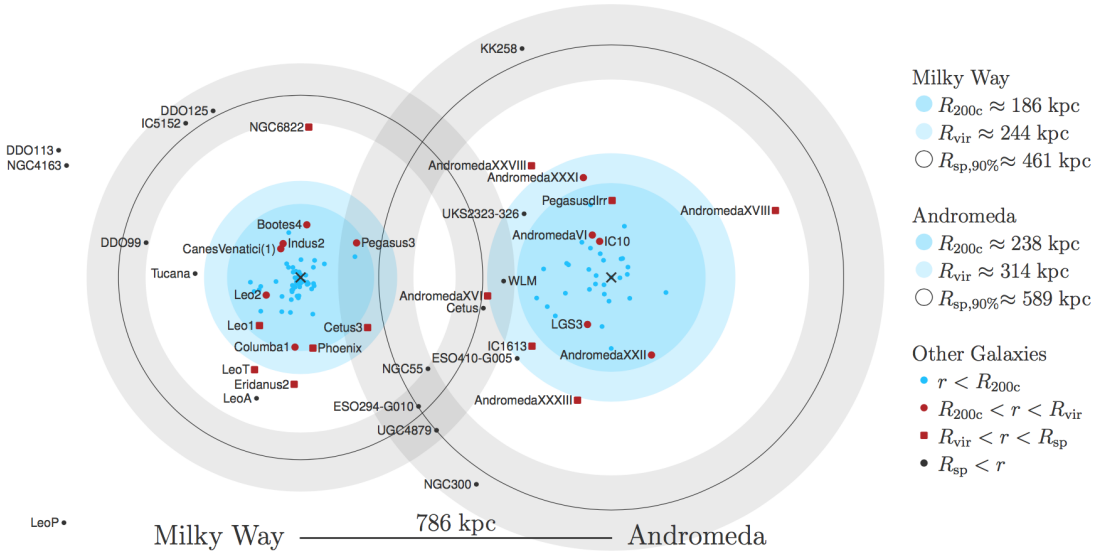

Figure 1.3: A view of the Milky Way-Andromeda system from Diemer (2021). Shows conventional spherical ovendensity radii and the splashback radius for both halos, R_{spl}. Many satellites typically thought of as outside the span of our galaxy, could be interpreted as subhalos if we choose a more encompassing radius like the splashback radius.

We mine Illustris-3, Illustris-3 Dark, Illustris-2 and Illustris-1 (to $z = 0$) for flybys and mergers throughout time and characterize the broad characteristics of the two types of interactions across time. Cosmological simulations provide ideal conditions to study flybys in many different environments and across a large mass range. Given the Illustris-3 and Illustris-3 Dark realizations we are able to study the effects that baryons have on the rates of both mergers and flybys. We also inspect the effect resolution plays on our search for flybys. Finally, we publicly release the full interaction networks for each of the simulations mined.

1.3.3 Halo and Subhalo Boundaries

As described above, the dark matter halo is an expansive and nebulous cloud of material surrounding galaxies. There is no clear boundary between where the halo begins and ends, so there are a multitude of options that are commonly used in the literature. In simulations where discrete particles are used to outline the distribution of matter, a common way to

define a halo is using the Friends-of-Friends algorithm (Davis et al., 1985). A fixed linking length is chosen and all particles within a linking length of another particle are ascribed to a halo. We call this the FoF halo. The FoF halo has no prior assumption of shape, but its edge density is set by the choice of linking length.

However, we know halos to be hierarchical in formation and structure, which means that inside a FoF halo, a family of subhalos may also exist. Subhalos exist as small bound substructures that appear as further overdense regions inside the background FoF, and may contain their own galaxy. A common choice for identifying subhalos is the use a spherical overdensity definition. Spherical overdensity definitions search for a uniform radius that encloses an overdensity equal to a fixed multiple of either the critical or matter density of the universe. These are relatively simple to compute and result in subhalos being defined as spheres with constant radii. Choices such as $R_{200,mean}$, $R_{200,crit}$, R_{vir} are commonly used (Press & Schechter, 1974; Lacey & Cole, 1994), but can be difficult to determine the exact edge of a subhalo that exists inside a FoF's which can have varying interior densities. Another limitation of this definition is that it assumes spherical symmetry for subhalos. The splashback radius, R_{spl} is another common choice Diemer (2021), but is difficult to compute and also describes a sphere.

Figure 1.3 shows several popular radial definitions for the Milky Way-Andromeda system. Known satellite galaxies are plotted as dots within either system. The choice of radius for either system would determine whether many of these galaxies are considered independent systems or substructure of the greater halos. Depending on where these galaxies are in their orbit with the host, they could be interpreted as flyby galaxies or simply as merged subhalos.

A large number of subhalo finding algorithms exist to identify these substructures. The Illustris simulation, employs a popular prescription called SUBFIND (Springel et al., 2001). An example of the SUBFIND halo algorithm in action is shown in Figure 1.4. Here we can see what the true distrubtion of particles and substructure looks like in the first panel

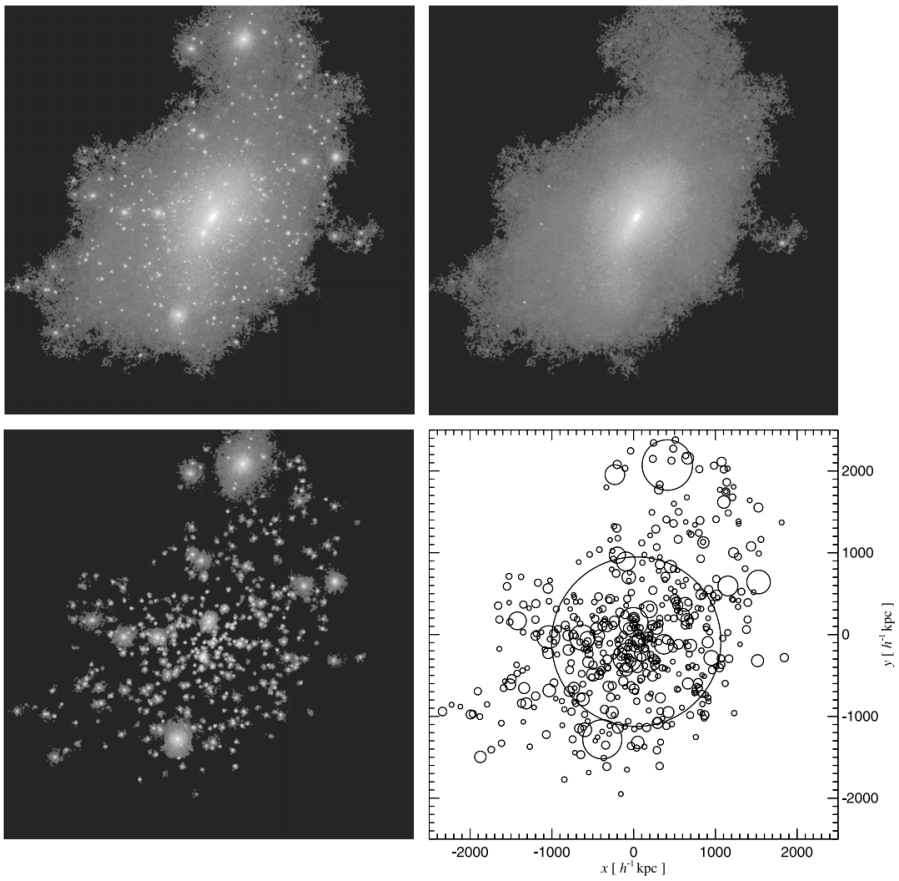

Figure 1.4: As seen in Springel et al. (2001) the SUBFIND algorithm is a popular method for identifying substructure of a halo. The full halo and its substructure is pictured in the first panel. The second shows only the background halo, or the FoF, followed in the third panel with only the subhalos. The final panel of the plot replaces the particles altogether with circles proportional to the number of particles present.

of the plot. The proceeding panels show the isolated FoF halo and the 495 subhalos. In the last panel, the particles are replaced altogether and the halos are illustrated as spheres, which due to the natural asymmetry of halos makes the expanse of subhalos appear far outside of the defined radius of the host.

Due to the varying nature of how we define the FoF and the subhalos, common properties such as mass and radius can be difficult to assign continuously as that halo changes status from being isolated to being accreted and existing as a subhalo of a separate structure. Because of this, to smoothly track these properties we choose to only pull halos from the Illustris subhalo catalog, and only reference the FoF for characteristics specific to the halo family as a whole.

The identifying characteristic of a flyby is that two previously independent halos become bound (one a subhalo of another) for some time, after which they return to being defined as independent halos. As we are using subhalos for the basis of our search, we separate centrals as the largest subhalo, comprised of the background particles of the FoF which are not bound to other subhalos (see panel 2 of Figure 1.4). The specifics of this process will be revisited in Chapter 2 of this thesis.

It is important to keep in mind that halos are defined based on definitions of choice, and each choice is associated with advantages for simplicity or computational expense, but none wholly encapsulate the reality of the structure.

1.4 Flybys and Backsplash Galaxies

1.4.1 Flybys

A *flyby* occurs when the dark matter halos of two independent galaxies interpenetrate and then detach forever. Figure 1.5 shows an example from a dark matter only cosmological simulation (Sinha & Holley-Bockelmann, 2011). Though the duration of a flyby may be fast, the perturbations induced can generate long lasting changes both in the intruder and the victim, similar to the effects of a minor merger (Sinha & Holley-Bockelmann, 2011;

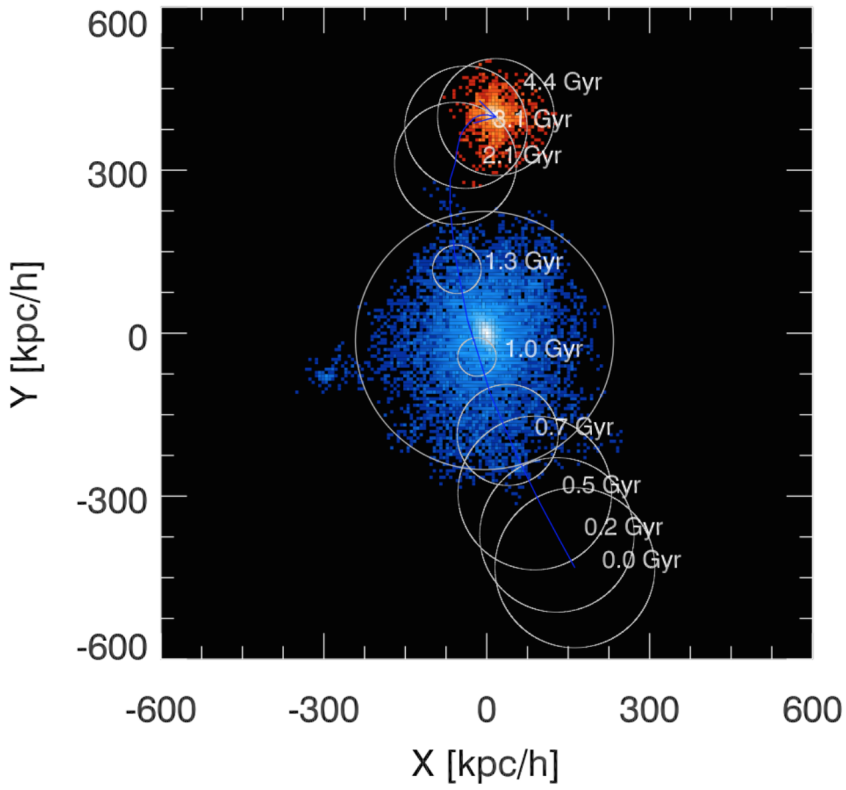

Figure 1.5: A 5:1 mass ratio flyby over 4.7 Gyrs as seen in Sinha & Holley-Bockelmann (2011). The host shown in grey is a Milky Way mass halo, and the flyby halo is successfully tracked as it enters and re-emerges from the other side. Shrinking of the radius is seen as the secondary passes through the host as a pseudo-evolutionary side effect of the secondary passing through the dense background of the host.

Lang et al., 2014; Vesperini & Weinberg, 2000).

Flybys have been invoked in several instances to account for mysterious changes in galaxies. They have been pointed to as a potential cause of excitation of spiral arms in the galactic disk (Tutukov & Fedorova, 2006), evolution of a spiral into an S0 galaxy (Bekki & Couch, 2011), or extra starbursts needed to explain abundances in massive ellipticals (Calura & Menci, 2011). Flybys could also be contributors to halo assembly bias (Gao et al., 2005; Wechsler et al., 2006). Halo assembly bias implies that the clustering of halos depends upon parameters other than halo mass alone. Ultimately, we want to further explore how the full interaction history transforms the physical properties of galaxies.

Isolated dark matter simulations have shown the power of flybys to create long lasting bars in galaxies depending on the orbital parameters as well as the mass ratio (Lang et al., 2014). An example of bar formation from a recent flyby encounter is seen in Figure 1.1 which shows the effects of a bar present 4 Gyrs after pericenter. Lang et al. (2014) found that the mass ratio of the interaction was crucial to the changes induced, with bar strength increasing in the secondary and decreasing in the primary as the difference in mass is increased.

However, the overall frequency of flybys is relevant to know how crucial they are in the cosmological picture of galaxy evolution. Sinha & Holley-Bockelmann (2011) studied flybys in a cosmological context using dark matter only simulations run to $z = 1$. Figure 1.6 illustrates the relevance of flybys to the cosmological picture by comparing merger and flyby rates across time and halo mass. For halos at low redshift ($z < 2$) flyby rates for halos with mass $> 10^{11} M_{\odot}$ show similar rates of flybys to mergers, and in some cases even favoring flybys as the dominant interaction type.

1.4.2 Backsplash Galaxies

Lately, there has been an ongoing conversation on the topic of "backsplash galaxies," or galaxies which are falling into another halo but on first passage may appear as a flyby

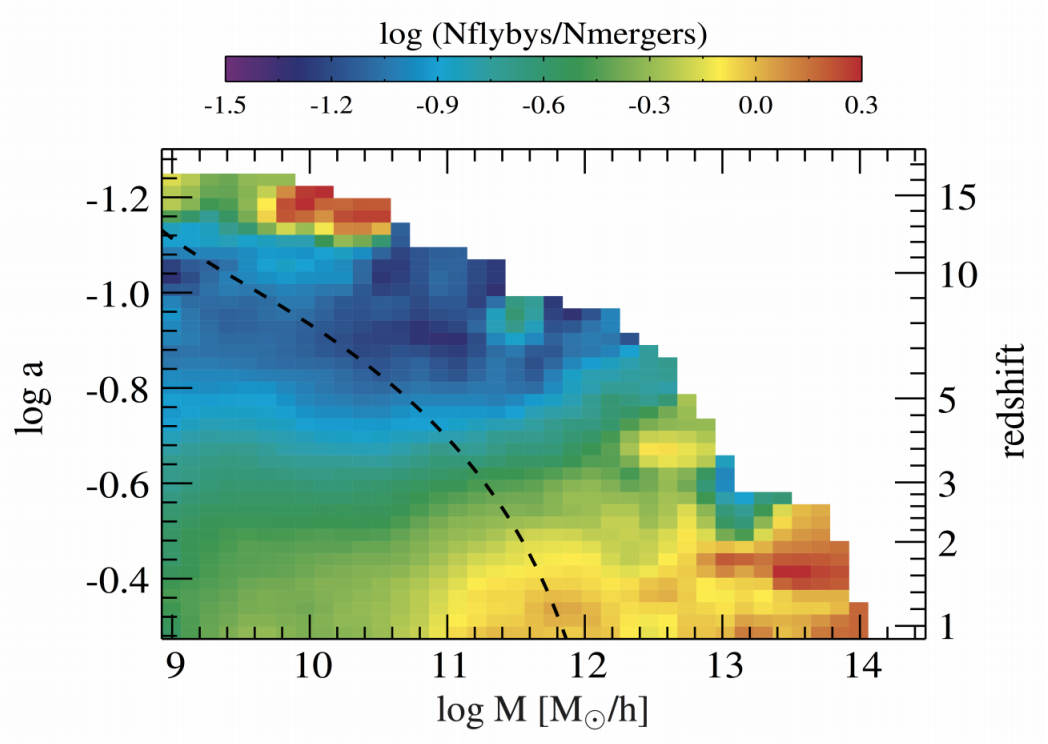

Figure 1.6: Relative rates of flybys and mergers as a function of scale factor, a, and halo mass as found in Sinha & Holley-Bockelmann (2011). The dashed line indicates the evolutionary path of a Milky Way mass halo. For massive halos ($> 10^{12} M_\odot$) after $log(a) \sim -0.4$ flybys rival mergers in frequency.

before splashing back and falling back onto the host. Diemer (2021) has shown that by defining a splashback radius, R_{spl}, which encompasses all material inside the turnaround point gives a more natural halo boundary.

Backsplash galaxies are thought of as galaxies or halos falling onto a larger host who do not immediately sink inwards, but pass inside a defined boundary and then exit before eventually falling back onto the host. Several groups have examined flybys and backsplash galaxies and have noted that the effects extend well outside of the spherical overdensity boundary. This has been seen in both observations (Pimbblet, 2011; Buck et al., 2019) and simulations (Wetzel et al., 2014; Haggar et al., 2020a; Knebe et al., 2020). Galaxies can be quenched and reddened out to $2R_{vir}$ (Balogh et al., 2000; Mamon et al., 2004). Others have found that the population of galaxies that have had a close encounter and are later found outside their hosts are kinematically distinct from others which have not had a close encounter.

Diemer (2021) has shown that by extending the boundary beyond the spherical overdensity radius of the host results in fewer flybys and more subhalos, and thus the choice of definition is critical in order to find agreement. Whether these halos are categorized as being in the greater splashback region of a host halo or as flybys who have previously had a close encounter has little importance on the effects seen by the galaxies themselves. However, calculating merger rates and flyby fractions can be keys to probing different aspects of cosmology (Diemer, 2021). They may also undergo transformations due to tidal stripping that create an overall redder population of quenched satellites surrounding massive galaxies (Wetzel et al., 2014).

1.5 Summary

This thesis further explores which interactions are common throughout the universe by using cosmological hydrodynamic and dark matter only simulations. We investigate which halo masses are likely to be involved in either encounter as well as which cosmic epochs are

prone to either type of interaction. By mining several realizations of the Illustris simulation we are able to compare the effects of baryonic physics and resolution have on halo to halo interactions. We study properties such as velocity, mass ratio, and proximity of either type of encounter to characterize the differences between the merging and flyby halo population. As a result, we publicly release our halo interaction network in an online catalog for others to further explore the effects of these encounters. By better understanding the differences between these types of interactions we can gain a more complete view of how galaxies and their halos evolve and take shape over the age of the universe.

Chapter 2

FINDING FLYBYS IN THE ILLUSTRIS SIMULATION

The following work will be submitted to the Monthly Notices of the Royal Astronomical Society Journal and is reprinted below in its entirety

Finding Flybys in the Illustris Simulation

Christina Davis[1], Kelly Holley-Bockelmann[1], Manodeep Sinha[2]

[1] Department of Physics and Astronomy, Vanderbilt University, Nashville, TN 37235

[2] Centre for Astrophysics and Supercomputing, Swinburne University of Technology, Hawthorn, Victoria 3122, Australia

2.1 Abstract

The lifespan of a galaxy is punctuated by both mergers and flybys, yet most methods to track the galaxy assembly history within a cosmological simulation are designed to identify only mergers. Here, we present the full halo interaction network for several runs of the Illustris simulation suite, available as a value-added catalog for the community. We describe the method to pinpoint both mergers and flybys, outline the features of the catalog, and identify differences and characteristics exhibited by the different interaction types. We find there are two distinct epochs during the age of the universe, the merger epoch (z=3 to z=1.5) followed by a flyby epoch (z=1.5 to the present) where flybys occur at similar rates as mergers. Mass ratios of flybys tend to less disparate than those of mergers. Flybys also happen at higher and less radial velocities, painting a picture of frequent grazing encounters on the outskirts of their companion. Lastly, the prevalence of flybys in simulations does not appear to be affected by the incorporation of baryons. We conclude that the presence of flybys cannot be ignored in the broader picture of galaxy evolution especially when studying galaxies near the present time.

2.2 Introduction

In a ΛCDM Universe, structure grows hierarchically, with small dark matter halos merging to accumulate mass that later become the larger halos that we see today. In the the classical picture, galaxies form within the dense centers of these halos (e.g. Ostriker & Peebles, 1973; Einasto et al., 1974). It is well-established that galaxy growth and evolution proceeds through a combination of galaxy mergers and smooth accretion of cold gas (Kereš et al., 2009). However, dark matter halo flybys may also influence the growth and evolution of galaxies within them (Weinberg, 1998). Not unlike mergers, flybys can perturb the underlying potential (Lang et al., 2014). In this paper we will present demographics of flybys in the Illustris simulation across time to better understand the role they may play in the evolution of galaxies and their host halos.

To understand how flybys could alter galaxy properties, we'll first discuss why mergers are seen as successful drivers of galactic evolution. For decades, it has been widely accepted that most galaxies have been influenced by merging at some point in their lifetime (Toomre, 1977; Barnes & Hernquist, 1992). Merger rates have been extensively studied both theoretically and observationally (Lacey & Cole, 1993; Guo & White, 2008; Genel et al., 2008, 2009; Hopkins et al., 2010b; Gottlöber et al., 2001; Angulo et al., 2009; Stewart et al., 2009). Simulations by Wechsler et al. (2002) estimate a Milky Way merger rate of roughly 10 interactions/Gyr at z=1.

It's been shown that mergers are able to transform the galaxy's morphology in a variety of ways, including destroying disks, creating bulges, or redistributing the stellar and gaseous components out to kpc scales (Holmberg, 1941; Hopkins et al., 2010a; Kormendy & Sanders, 1992; Naab & Burkert, 2003; Barnes, 2002; Larson & Tinsley, 1978; Clauwens et al., 2018; Athanassoula et al., 2016). Mergers also contribute to the formation and destruction of bars, boxy or peanut shaped stellar orbits, shells, tidal arms, and streams (Wild et al., 2014). Interacting galaxies may also trigger central starbursts via gaseous inflows. This enhanced star formation rate is reflected in the chemical enrichment of the ISM. While

the inner galaxy sees star formation enhancement, the outskirts are often left quenched (Moreno et al., 2015; Cox et al., 2006; Joseph et al., 1984; Hernquist & Mihos, 1995; Kennicutt et al., 1987; Bushouse, 1987; Barton Gillespie et al., 2003; Lambas et al., 2003; Nikolic et al., 2004). In addition, by depositing material into the galaxy, mergers can fuel supermassive black holes (Hopkins et al., 2005, 2006; Micic et al., 2007; Heckman et al., 1986; Micic et al., 2011; Younger et al., 2008). Indirect evidence of this link can be seen with active galactic nuclei (AGN), which are seen at higher fractions in galaxies with a recent major merger than within the general galaxy population (Schweizer, 1986; Mihos & Hernquist, 1996; Moore et al., 1996; Dahari, 1984; Springel et al., 2005; Weigel et al., 2018). In turn, the feedback from this black hole fueling episode is a key ingredient in regulating star formation throughout the galaxy host (Martín-Navarro et al., 2018).

It is clear that mergers have a wide range of influence over the evolution and transformation of galaxies, however, this cosmological perspective neglects another type of dynamical interaction – flybys. Flybys are halo-halo interactions in which a secondary halo (or intruder) is able to escape the potential of a primary halo (or victim) after an encounter. Flybys have been found in dark matter only cosmological simulations (Sinha & Holley-Bockelmann, 2011) and have been shown to have the potential to dynamically perturb the involved halos (Sinha & Holley-Bockelmann, 2015). While flybys are defined as halo-halo interactions, the galaxies within may also be altered dramatically. Weinberg (1998) showed that a resonant interaction in the outskirts of a dark matter halo can cause perturbations to be carried to the central galaxy. Other groups have also verified the ability of skirting halos to alter the galaxy within the primary halo (D'Onghia et al., 2010; Tutukov & Fedorova, 2006; Bekki & Couch, 2011; Dubinski & Chakrabarty, 2009; Łokas, 2018). Simulations show that close flyby encounters can incite bars and warps in the interacting galaxies (Peschken & Łokas, 2018; Lang et al., 2014; Sinha & Holley-Bockelmann, 2015), which themselves can change the shape or potential of a dark matter halo (Holley-Bockelmann et al., 2005), create gas inflow into the galaxy, suppress star formation, and may help grow the central

supermassive black hole (SMBH) (Kormendy & Kennicutt, 2004; Laurikainen et al., 2007; Hu, 2008).

Several groups have found a quiescent population of galaxies out to several virial radii of the host (Wetzel et al., 2013), comprised of ejected satellites that will either escape forever or spend several Gyrs outside of the cluster before falling back towards the cluster center (Pettitt & Wadsley, 2018; Wetzel et al., 2014; Mahajan et al., 2011). This could indicate that flybys quench satellites as they pass through larger halos. It is a possibility that flyby encounters posses the power to transform galaxies in much the same way as minor mergers (Dubinski, 1999; Vesperini & Weinberg, 2000; Sinha & Holley-Bockelmann, 2015; Lang et al., 2014)

In this paper we present a complete census of all flybys and mergers in the hydrodynamic runs Illustris-1 (to z=1), Illustris-2, Illustris-3, as well as the dark matter only run, Illustris-3 Dark. We will inspect the frequency of mergers and flybys across time, as well as look at which mass halos are prone to each interaction. To better understand the physical properties of each population, we inspect the mass ratios, velocity distributions, and depth of penetration of our flyby population. We will also compare the prominence of each type of interaction between simulations to examine the effects of resolution and baryonic physics.

Table 2.1: The Illustris Simulation Specifications. N_{DM}, ϵ_{DM}, and m_{DM} state the number of dark matter particles, the softening length, and the particle mass. N_{Halos} indicates the total number of halos found at a particular time. We report values for $z = 1$ and $z = 0$ for all runs except Illustris-1 which was run down to $z = 1$. $N_{mergers}$ and N_{flybys} give the cumulative number of mergers and flybys found up until either $z = 1$ or $z = 0$.

Run Name	$N_{\rm DM}$	$\epsilon_{\rm DM}$ [kpc]	$m_{\rm DM}$ [$M_\odot$]	$N_{\rm Halos}$ ($z=1$)	$N_{\rm Mergers}$ ($z=1$)	$N_{\rm Flybys}$ ($z=1$)	$N_{\rm Halos}$ ($z=0$)	$N_{\rm Mergers}$ ($z=0$)	$N_{\rm Flybys}$ ($z=0$)
Illustris-1	1820^3	1.4	4.4×10^6	7.7×10^6	2.68×10^6	7.43×10^5	–	–	–
Illustris-2	910^3	2.8	5.0×10^7	8.3×10^5	6.3×10^5	9.1×10^4	6.9×10^5	1.1×10^6	2.1×10^5
Illustris-3 Hydro	455^3	5.7	4.0×10^8	2.3×10^4	8.7×10^3	2.1×10^3	2.3×10^4	1.76×10^4	8.19×10^3
Illustris-3 Dark	455^3	5.7	4.0×10^8	2.6×10^4	1.1×10^4	2.6×10^3	2.7×10^4	2.9×10^4	9.6×10^3

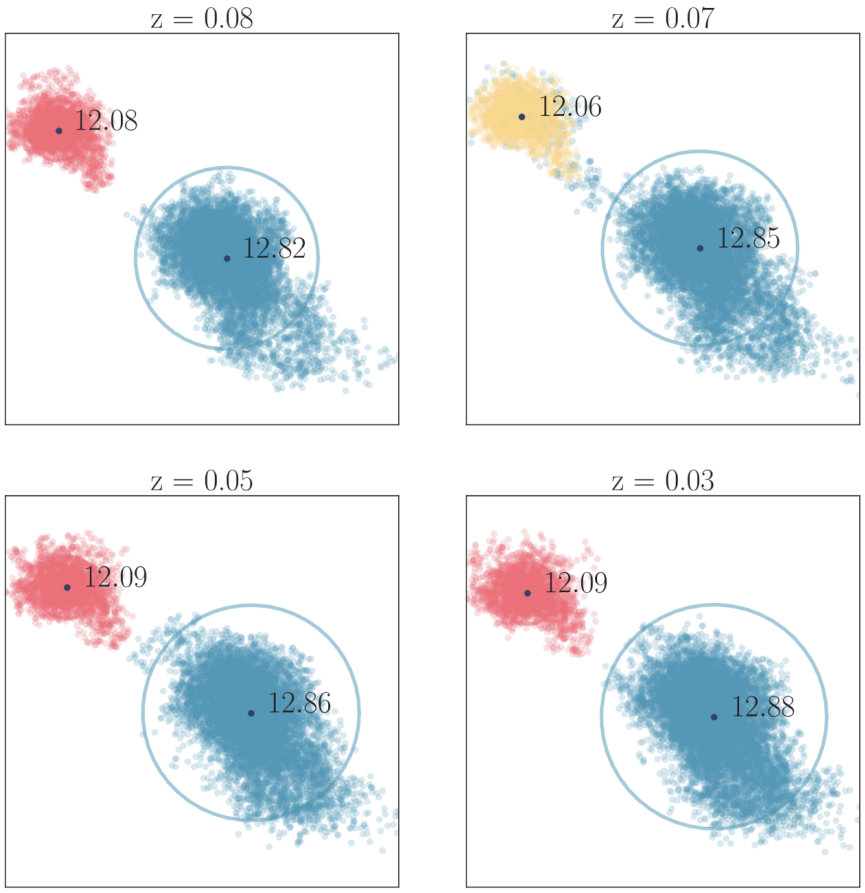

Figure 2.1: A flyby observed over 0.6 Gyrs in the x-y plane. The flyby occurs in the second pane, where the secondary halo is colored yellow. The instantaneous dark matter halo mass is annotated as $\log(\text{Mass}_{halo})$. Rings show the radius, $R_{mean,200}$ of each halo.

2.3 Data and Methods

We construct the complete interaction history of each resolved halo in Illustris-3, Illustris-3 Dark, Illustris-2, and Illustris-1 (to z=1) with the addition of flyby tracking. In this section we outline general properties of the Illustris simulation and how the data are handled to create the database. We will also discuss the `HINGE` framework that is used to identify flyby interactions.

2.3.1 The Illustris Simulation

Illustris is a suite of high resolution, cosmological hydrodynamic simulations of a $(106.5\text{Mpc})^3$ volume (Nelson et al., 2015; Vogelsberger et al., 2013). It employs the hydrodynamic code, AREPO (Torrey et al., 2013), which is based on an unstructured moving mesh. It evolves the box using a ΛCDM cosmology consistent with WMAP-9: $\Omega_m = 0.27$, $\Omega_\Lambda = 0.73$, $\Omega_b = 0.0456$, $\sigma_8 = 0.81$, $n_s = 0.963$, $h = 0.704$ (Hinshaw et al., 2012). There are three realizations of the volume at varying resolution, with Illustris-1 being the most refined. Details for each of the simulations can be found in Table 2.1. There are also three accompanying dark matter only runs available. We construct catalogs of the full interaction network for Illustris-1 to z=1, and Illustris-2, Illustris-3, and Illustris-3 Dark to z=0. Illustris includes the physics of star formation and evolution, a stellar feedback prescription, primordial and metal-line cooling with self-shielding corrections, gas recycling and chemical enrichment, black hole seeding and growth, as well as the accompanying AGN feedback. The implemented physics has been shown to reproduce many observed physical scaling relations (Vogelsberger et al., 2013). The Illustris Simulation is meant to capture the physics of many different processes at a large range of scales, but it has a few noted drawbacks with respect to the AGN and stellar feedback models. It's been shown to have too high a cosmic star formation rate density as well as too high a stellar mass function at high redshifts, and finally the total gas inside R_{200} is considered to be too small. All of these are clues that the feedback prescription is too violent in some regimes, or that quenching and cooling mechanisms are not efficient enough to reproduce known relationships. Another point to be aware of is that the spatial extent of galaxies can be a factor of a few higher than what we observe at $M_\star < 10^{10.6} M_\odot$ (Vogelsberger et al., 2014; Snyder et al., 2015; Genel et al., 2014). Note that IllustrisTNG alleviates many of these problems with a new galaxy formation model (Pillepich et al., 2017; Weinberger et al., 2016). Many of these shortcomings have direct implications for the baryonic properties of the simulation, but we are primarily concerned with dark matter halo tracking. We show that Illustris-3

and Illustris-3 Dark to have extremely similar interaction demographics and conclude any drawbacks in the particular hydrodynamic prescription has little effect on our results.

Halos are identified first using a friends-of-friends (FoF) technique with a linking length of $b = 0.2$ (Davis et al., 1985). Subhalos are identified using the SUBFIND algorithm (Springel et al., 2001). In the Illustris database, FoF halos are assigned when a halo has more than 32 linked particles. The SUBFIND technique uses an adaptive kernel interpolation to identify locally overdense regions in a given density field. These overdense regions are assigned a boundary given by the first isodensity contour that passes through a saddle point in the density field. After identification of a prospective subhalo, unbound particles are removed and assigned to the central subhalo. We will call this the primary subhalo. For the purpose of identifying flybys, we choose to require a halo to contain at least 100 dark matter particles to be considered well-defined. This makes our smallest halo masses $4.4 \times 10^8 M_\odot$, $4.4 \times 10^9 M_\odot$, $4.0 \times 10^{10} M_\odot$ for Illustris-1, Illustris-2, and Illustris-3 respectively, thus any halos below these mass thresholds are not included in our interaction network. Gas, star, and tracer particles are given the halo membership of their closest dark matter particle. Halo catalogs for the Illustris simulations are available through their online API (https://www.illustris-project.org/data/docs/api/).

The largest subhalo in a given FoF group represents the central subhalo and all subsequent subhalos are to be considered satellites, all of which are contained within the parent FoF halo. Since the procedure for identifying FoF halos is separate from subhalos, many fundamental properties such as mass and radius are computed differently. As we are concerned with tracking these properties of halos as they change status between central and subhalo, we choose to exclusively use data from the subhalo catalog and adopt the central subhalo as the **central halo**. All other subhalos identified in that FoF family are considered to be satellites or **subhalos** of the central halo. The only property inherited from the FoF halo is the group radius, for which we choose to use $R_{200,mean}$ representing a comoving radius of a sphere whose mean density is 200 times the mean density of the Universe. All

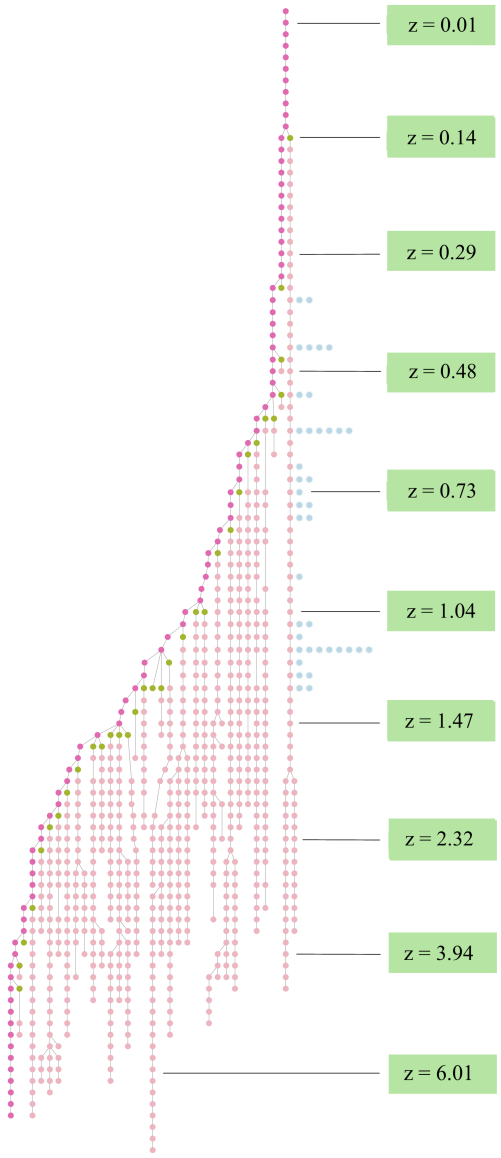

Figure 2.2: A merger tree showing the assembly of a halo with $M_{halo} = 10^{11} M_{\odot}$ at $z = 0$. The hot pink dot along the left hand side of the tree represents the main halo at each time step. All green dots represent other independent halos that are about to merge with the main halo, and blue dots along the side show flybys with the main halo. Each light pink dot shows progenitors of each halo that is merged to create the final halo at $z = 0$.

halo masses are taken from the Illustris subhalo catalog, which identifies a halo's mass as the total mass of all particles which are bound to the subhalo, and no other subhalo. This is a useful scheme as each particle only has membership to one subhalo at a time. Any given particle is either a member of a bound satellite subhalo or part of the background making up the FoF and is therefore associated with the central subhalo. All halos in our sample have a listed half-mass radius taken from the Illustris online database, as well as a virial radius computed from the particles themselves. Each of these radii are included in the online database. We choose to report the proximity of halos during pericenter passage based on the parent FoF's $R_{200,mean}$ as it represents an extent of the halo based on all enclosed mass including all subhalos who are members of that halo family. All references to which Illustris FoF a given subhalo is associated are preserved in the online database discussed later in the text. There are many options for choice of radius, however, our results are independent of this choice as radius is not a criterion used to assign flybys.

2.3.2 Identifying Flybys

To identify flybys, we construct a full interaction network for each halo that looks at all dynamical interactions the halo experiences. We use the `HINGE` framework described in Sinha & Holley-Bockelmann (2011) to build the interaction network, and we summarize the framework below. `HINGE` is a three-part algorithm that tracks halos across time and identifies different interaction scenarios while correcting for several persistent problems in halo misidentification.

The first part is `haloparentfinder`, which is responsible for tracking halo IDs across time. For each halo in a given snapshot, we inspect the next snapshot in order to identify the corresponding halo with the most particles in common; we call this the parent halo. This matching scheme is performed on every halo at a given snapshot until all possible halo IDs are matched with halos in the future snapshot. To identify merging halos, many halos from the starting snapshot may match with a single parent in the subsequent snapshot. Parent

halos having multiple children is a consequence of both merging and flybys.

The scheme for subhalos differs because a sizeable amount, even a majority, of a subhalo's particles can be stripped when entering a tidal field. Even if most of the outer particles are stripped, we would like to recover the parent of the highly stripped core, so `HINGE` uses a binding energy rank to weight each particle by its potential. This prioritizes highly bound particles that are shared between parent and child pairs to correctly assign the progenitor. Boylan-Kolchin et al. (2009) uses a similar method to track cores of stripped subhalos.

The second piece of `HINGE` is `orphanfixer`, which is meant to fix another insidious problem related to SUBFIND or any density-based subhalo algorithm. Subhalos within background halos are identified as regions of higher density relative to the background, but as the subhalo moves deeper into the parent halo, the background density increases and the subhalo artifically shrinks and may be lost for a number of snapshots as it passes the center of the host (Muldrew et al., 2011). This is a well-known problem that can cause errors in an interaction network by mislabeling the reappearance of a subhalo as a new subhalo with no parent, or orphan. To correct for this, `orphanfixer` looks for parent matches beyond the moment of reappearance to see if it is a known subhalo that has been artificially disrupted.

The final piece of the framework is `mergertree` which builds the interaction network in full and identifies different interaction scenarios. We are able to separate flybys from various types of mergers for every halo throughout the simulation, whether or not they survive to $z = 0$. More details and code can be found https://github.com/manodeep/hinge.

We identify the following categories of interaction:

1. Subhalo Mergers, in which a central halo falls into another central halo and survives as a subhalo until z=0.
2. Complete Subhalo Disruption, follows the same entry as (1) but is disrupted any time after merger and falls below our mass resolution into the central halo.
3. Flybys, a central halo temporarily becomes a subhalo of another central, but then

returns to being its own central at a later point in time.

   (a) Pure Flybys, a special case of a flyby interaction where the intruder in the flyby encounter does not end in a merger with the primary at any later point in time.

   (b) Merging Flybys are the remainder of the flyby category, in which the halos engaged in a flyby interaction end in subhalo merger at a later time.

4. Disappearing Halos, where one central halo falls below our mass threshold as it is falling into another halo and never becomes a subhalo. These halos are excluded from the interaction catalog of merging and flyby halos.

We created full interaction networks for Illustris-3, Illustris-3 Dark, Illustris-2, and Illustris-1 (to $z = 1$) which we have published online. This includes information on every interaction itemized above for each halo throughout the simulation.

Figure 2.2 shows a sample merger tree of a $M_{\rm halo} = 10^{11} M_{\odot}$ halo from Illustris-3 Hydro that exists at $z = 0$. The main halo can be followed backwards in time as can all halos that contributed to its assembly through merging directly with the main halo. Halos about to merge at the subsequent snapshot are colored in green with their progenitors in light pink, and flybys are illustrated off to the side in blue. Since their entire mass is not permanently deposited into the primary we do not include their progenitors as part of the merger tree for the final halo at $z = 0$. You can see that at several snapshots of this particular halo, there are more flybys than mergers. The frequency of flybys also increases for this halo beyond $z \sim 1.5$ until the halo finds itself in a relatively quiet phase until $z = 0$. Each halo has a unique assembly history which can look vastly different, but information such as mass, radius, hierarchy levels, progenitor IDs, and interaction types are stored in our database which will be discussed more in depth later in the text.

Before continuing, we must acknowledge one classification of interactions that are not included in the final analysis. We impose a particle number requirement of 100 dark matter particles. Because of this, a halo right above this limit could be considered a central halo for a time, but particle noise, stripping, or other interactions could cause the halo to

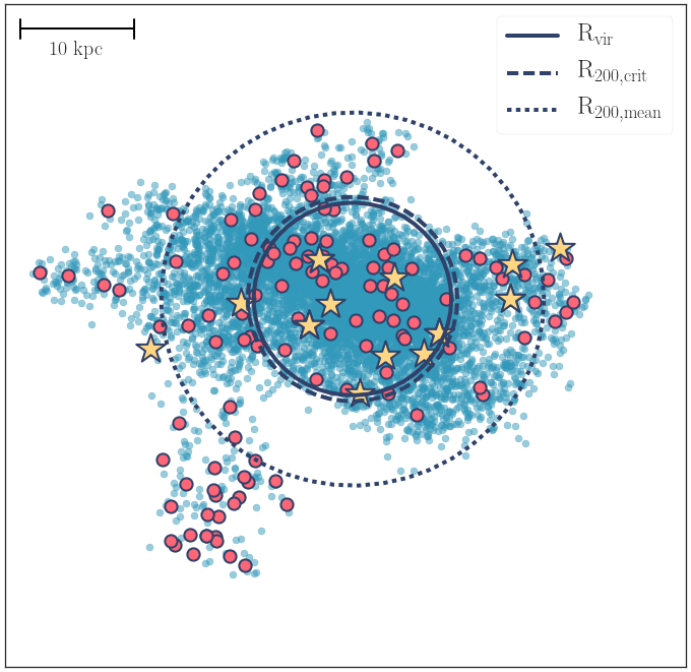

Figure 2.3: A massive $10^{14} M_{\odot}$ halo from $z = 0$ in the Illustris-3 simulation. Light blue points show particles associated with the central halo and dark blue circles show different spherical overdensity radius definitions. Pink dots show the center of mass of all subhalos of this central at this time and yellow stars indicate the center of mass of surviving halos who experienced a flyby with the central at some point in their history. The central halo is highly non-spherical resulting in subhalos found outside of its radius, regardless of which radial definition is chosen.

fall below our imposed particle threshold and disappear from our catalog. Some halos in our simulation disappear immediately upon entering a neighboring halo. As other groups have shown that it is unlikely that halos disrupt entirely upon interacting (van den Bosch et al., 2017), it is much more likely that a fraction of its particles are stripped but a core remains below the resolution limit. Whether this core will end in a merger with a remaining subhalo, complete dissolution, or a flyby is unclear, so we exclude these from our merger and flyby counts, and simply dub them *disappearing halos*. However, halo IDs and relevant physical information is stored in the database at all times in which they meet the 100 particle threshold.

Disappearing halos primarily affect the lowest mass bin of any given simulation and convergence with higher resolution simulations is reached quickly after increasing mass by half an order of magnitude. This means that for Illustris-3, even though halos of mass $4.0\times 10^{10} M_{\odot}$ are resolved, many of these halos are lost upon engaging in an interaction. Thus our flyby and merger counts for halos between $4.0\times 10^{10} M_{\odot}$ and $9.0\times 10^{10} M_{\odot}$ for Illustris-3 are only complete to 50%. Similarly, for Illustris-2 we reach convergence with Illustris-1 by $9.0\times 10^{9} M_{\odot}$. Beyond the range close to the resolution limit for each simulation, counts for both flybys and mergers agree remarkably well when using mass cuts to compare with varying resolution.

2.3.3 Backsplash Galaxies

Lately, there has been a focus on “backsplash galaxies," galaxies or halos which have passed through a group or cluster and are found outside the primary. They are usually found within the splashback radius, $\sim 2R_{vir}$ of the central, and will perhaps eventually end in a complete merger after losing kinetic energy following each passage (Pimbblet, 2010; Wetzel et al., 2013; Ludlow et al., 2009). Although there is some affinity between what we call flybys and backsplash interactions, the critical difference is that a flyby describes one encounter which does not result in the immediate and permanent merging of two halos.

Instead the interacting halos become unbound for some time after the encounter. Flyby halos must temporarily become a subhalo of another halo, then return to being a central. Many flyby halos may subsequently find themselves in the splashback region of the cluster, but they must not remain a subhalo of another central in order to be identified in our work as a flyby (Balogh et al., 2000; Mamon et al., 2004).

Diemer (2021) and More et al. (2016) have advocated for the adoption of the splashback radius, R_{sp}, over commonly-used spherical overdensity radii such as R_{vir} or R_{200} which fail to capture many physical differences between halos. The splashback radius is defined as a sharp drop in density in the halo outskirts, beyond the pile up of accreted material that has reached its first apocenter. This physically motivated radius conveniently divides orbiting material from infalling material (Fillmore & Goldreich, 1984; Bertschinger, 1985; Lithwick & Dalal, 2011; Vogelsberger & White, 2011; Adhikari et al., 2014; Shi, 2016).

Diemer (2018) and More et al. (2015) have created techniques to identify the splashback radius around halos which takes into account the density of a halo's surrounding material (Mansfield et al., 2017). The splashback radius of a halo is dependent upon a variety of factors including accretion rate, matter density of the universe, and shape of the halo itself. More et al. (2015) showed that the splashback radius for a rapidly accreting halo could be up to $2R_{200,mean}$ but this is by no means a universal size and requires an expensive, in-depth assessment of each halo to determine a true 3D boundary. Our approach avoids the usage of a radial boundary in order to separate centrals from satellites. We instead use hierarchy information from the halo finder to determine if a halo is bound to a larger structure.

It is important to point out that the physical extent of a subhalo population is expansive – subhalos can be bound at radii above $2R_{200,mean}$. This is primarily because the $R_{200,mean}$ radius is based on a spherical profile, while halos can be asymmetrical. As seen in Figure 2.3 a significant distribution of particles can extend outside of the $R_{200,mean}$ boundary. Using a definition based on subhalo membership, we avoid any bias in the shape of the central halo.

Identifying flybys by our definition within the splashback region will likely not account for all galaxies that are considered “backsplash galaxies" since many may remain bound as subhalos to $z = 0$ or until a final merging event, even when outside $R_{200,mean}$. This means that by scanning the halos inside the splashback region will result in finding some flybys as well as some bound halos, and not all flybys will remain in this region. As shown in Haggar et al. (2020b) most galaxies which have dipped inside the R_{vir} radius of the halo, can be found inside 1-2 R_{vir} at $z = 0$. While some may identify these as “flybys" using radial spherical overdensity boundaries, these halos are unlikely to return to being a central halo after the interaction and therefore would not be considered flybys by our definition. This is due to the fact that the typical subhalo population extends well outside of R_{vir}, which results in most flyby interactions also happening outside of this boundary.

Diemer (2018) shows that using a radial definition to differentiate bound and unbound halos will result in boundary-crossing errors when the radius is drawn inside the orbital apocenter of accreted material. He recently posited that most flybys are simply misidentified satellites caused by oscillating around an arbitrary radial boundary and should instead be seen as satellites throughout their orbit of the central. Choosing to use a spherical overdensity radial boundary will almost always result in an under-counting of subhalos and and an over-counting of flybys. As shown in Diemer (2018), this choice of a spherical boundary can drastically change the flyby and subhalo fraction.

In Figure 2.4 we show the flyby fraction as a function of secondary halo mass. As pointed out in Diemer (2018), a larger, more inclusive halo boundary tends to lower the flyby fraction compared to its spherical overdensity counterparts. We find the highest flyby fraction from Illustris-1 to be 0.8% for halo masses of $4 \times 10^9 M_\odot$. Diemer (2018) find a similar flyby fraction when using the splashback radius encapsulating 90% of material, $R_{sp,90\%}$, as their separating radius. This implies that while our definitions of flyby are not the same, we do not expect to be severely over-counting flybys which are merely the first passage of a merger.

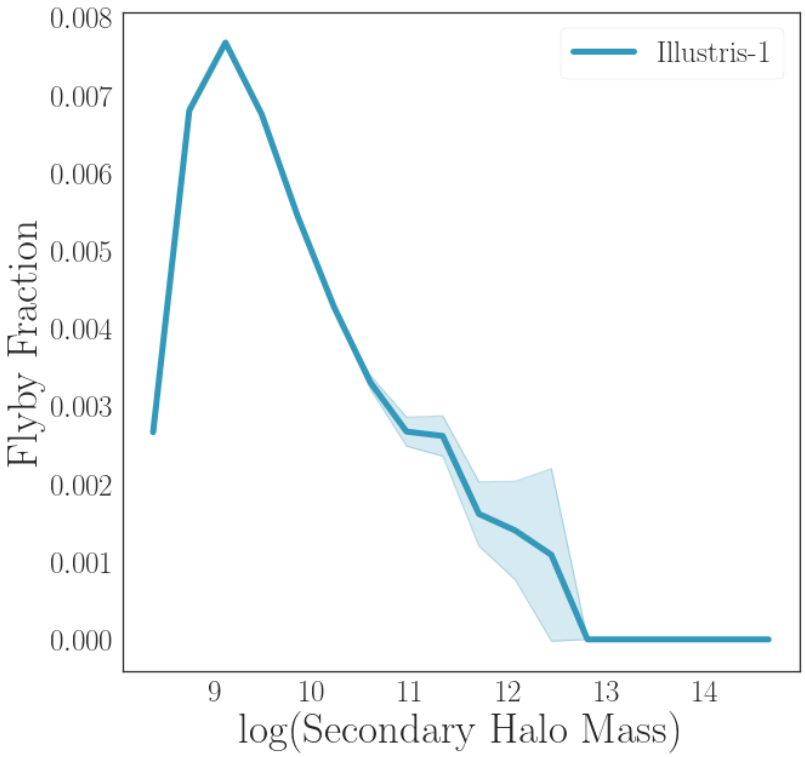

Figure 2.4: The fraction of all halos who have been the secondary in a flyby interaction as a function of halo mass for Illustris-1. We see flyby fraction is a function of mass, with up to 0.8% of dwarf-sized halos experiencing a flyby during their lifetime.

No method for identifying skirting satellites will be perfect as it is always subject to some boundary. However, in our case, it is not a radial boundary, but the potential boundary as determined by SUBFIND. This will inevitably result in some halos close to the edge of a larger halo to vacillate between being categorized as a bound satellite or a central halo of its own between snapshots. Our tagging scheme will find many of these edge-case halos and tag them as flybys due to their central-satellite-central transition. This is not seen as contamination to the flyby population, since these halos indeed qualify as halos who come close enough to experience some perturbing effects of another primary halo and yet escape its gravitational influence, at least temporarily.

2.3.4 Online Catalog Structure

We created a shareable census of all the halos used in this analysis organized in an online catalog. For Illustris-3 Dark, Illustris-3, Illustris-2, and Illustris-1 (up to $z = 1$) we traced all halos above our particle resolution throughout time and chronicled each interaction with other halos. Each simulation includes two corresponding columnated data files: one which records all halos in the snapshot with various physical properties, and the other which contains exclusively central to subhalo merging events and flybys.

The halo catalog contains properties listed in 2.2. All halos in our catalog are downloaded from the *Subhalo Illustris* database to smoothly keep track of halo identity and properties as it changes from being a central to a subhalo across time. Halo IDs are assigned such that each halo can be uniquely identified across snapshots, but corresponding Illustris IDs are listed to look up all other provided properties in the original database. Central halos assigned a hierarchy level of 1 while subhalos are given a 2. The number of subs gives the number of subhalos contained in our catalog belonging to this halo system, where satellite subhalos are given a value of 0. Center of mass positions, peculiar velocities, and half mass radii R_{hal} are given exactly as in the Illustris subhalo database. Illustris FoF ID,

Halo Property	**Units and Description**
Snapshot	Illustris simulation snapshot
HaloID	Uniquely assigned haloID, consistent across time
Halo mass	$[10^{10} M_{\odot}]$ Total mass of all particles belonging to halo
Hierarchy level	1: central, 2: subhalo
Nsubs	Number of subhalos belonging to this halo
R_{vir}	$[ckpc/h]$ Virial radius of the halo
R_{half}	$[ckpc/h]$ Half mass radius of the halo
$R_{200,mean}$	FoF's radius corresponding to mean density
$R_{200,crit}$	FoF's radius corresponding to critical density
x, y, z	$[ckpc/h]$ Center of mass position
v_x, v_y, v_z	$[km/s]$ Peculiar velocity of the halo
IllustrisID	the index into the Illustris Subhalo catalog for a given snapshot
FoFID	the IllustrisID for the FoF of a given halo

Table 2.2: Halo Catalog properties and descriptions. Data available in the online database for each processed simulation run.

and both FoF radii are properties of the parent FoF halo of the selected subhalo and are references to the Illustris FoF Halo database. The number of subs, N_{subs}, counts the number of subhalos belonging to the central subhalo that met our resolution threshold. It can be expected that these values do not correspond to the values in number of subhalos listed in the Illustris database since these refer to all halos inside of a parent FoF without our additional requirement of 100 particles.

The interaction catalog is stored in a separate columnated file since many halos can be repeated within a given snapshot if they experience more than one interaction in one timestep. Thus many halos will appear several times per timestep if they are experiencing simultaneous interactions, which is quite common for high mass halos. The interaction database is stored separately such that the full halo database can maintain a unique entry for each halo at a given time. This reduces the volume of data stored by avoiding repeats, and simplifies the process of looking up properties of a particular halo at a specific timestep

Halo Property	**Units and Description**
HaloID	HaloID of the primary, same as in Halo Catalog
Secondary HaloID	HaloID of the secondary, same as in Halo Catalog
Interaction Type	1: flyby, 2: merger
Halo Mass	$[10^{10} M_{\odot}]$ Mass of the primary halo
Secondary Halo Mass	$[10^{10} M_{\odot}]$ Mass of the secondary halo
Snapshot	Snapshot of infall where secondary is first a subhalo
Duration	Number of snapshots spent as a subhalo for flybys, mergers: -3
Distance Between	$[ckpc/h]$ Distance between the center of mass of primary and secondary
Infall Distance	$[ckpc/h]$ Distance between the center of mass of primary and secondary at time of infall
Pericenter Distance	$[ckpc/h]$ Total distance between the center of mass of primary and secondary
$R_{peri}/R_{200,mean}$	The pericenter distance given in terms of the FoF's $R_{200,mean}$
V_{rel}	$[km/s]$ Relative velocity between the primary and secondary
V_{esc}	$[km/s]$ Escape velocity at time of interaction
V_{rad}/V_{rel}	Component of V_{rel} pointed toward the companion

Table 2.3: Interaction Catalog properties and descriptions. Data available in the online database for each processed simulation run.

by returning only one result. We also allow a halo pair to have multiple flyby interactions at different times. A flyby is identified as an individual event where a halo changes status from central to satellite, back to central. This condition may be met multiple times as halo orbits its companion. It is also permitted that flyby halos may also eventually end in merger with the same primary. We define“pure flybys" and “merging flybys" to distinguish those halo pairs which do not merge with each other (though either halo may merge with a different halo later on).

This catalog only includes halos which are experiencing either a central to subhalo merger or a flyby which is tagged at the time of infall, the snapshot where it first becomes a subhalo. Interaction types are given values of 1 or 2 for flyby and merger respectively. The secondary halo is the halo that experiences the central to subhalo transition and the host of the interaction is considered to be the primary. It is usually the case that the primary is more massive than the secondary, but there can be exceptions for similar mass encounters. The duration is given in number of snapshots spent as a subhalo in the case of flybys, for mergers we have assigned an arbitrary value of -3 since mergers are situations where the subhalo either never escapes or dissolves inside the host. The pericenter distance is given in $[ckpc/h]$ as the closest distance between the centers of the primary and secondary during the period where the secondary is a subhalo.

2.4 Results

2.4.1 Flyby and Merger Abundance

To understand how influential flybys are to the cosmological evolution of galaxies we first want to know about their abundance, in particular how frequent they are relative to mergers and at which cosmic times. Figure 2.5 shows the number of flybys and mergers across time from each of the hydro Illustris runs. As the mass resolution for Illustris-1 is much finer, the total number of interactions of each type is significantly larger than the lower resolution simulations. We compare the simulations with a uniform mass cut in Figure 2.6. Because of the overwhelming number of halos at smaller masses, increasing the resolution causes the number of each type of interaction to grow substantially. This also causes the number of interactions in both flybys and mergers to begin rising at earlier times. In the context of hierarchical structure formation, this makes reasonable sense, as small halos will form earlier and begin merging until they reach a mass that can be resolved in the lower resolution versions of the simulations.

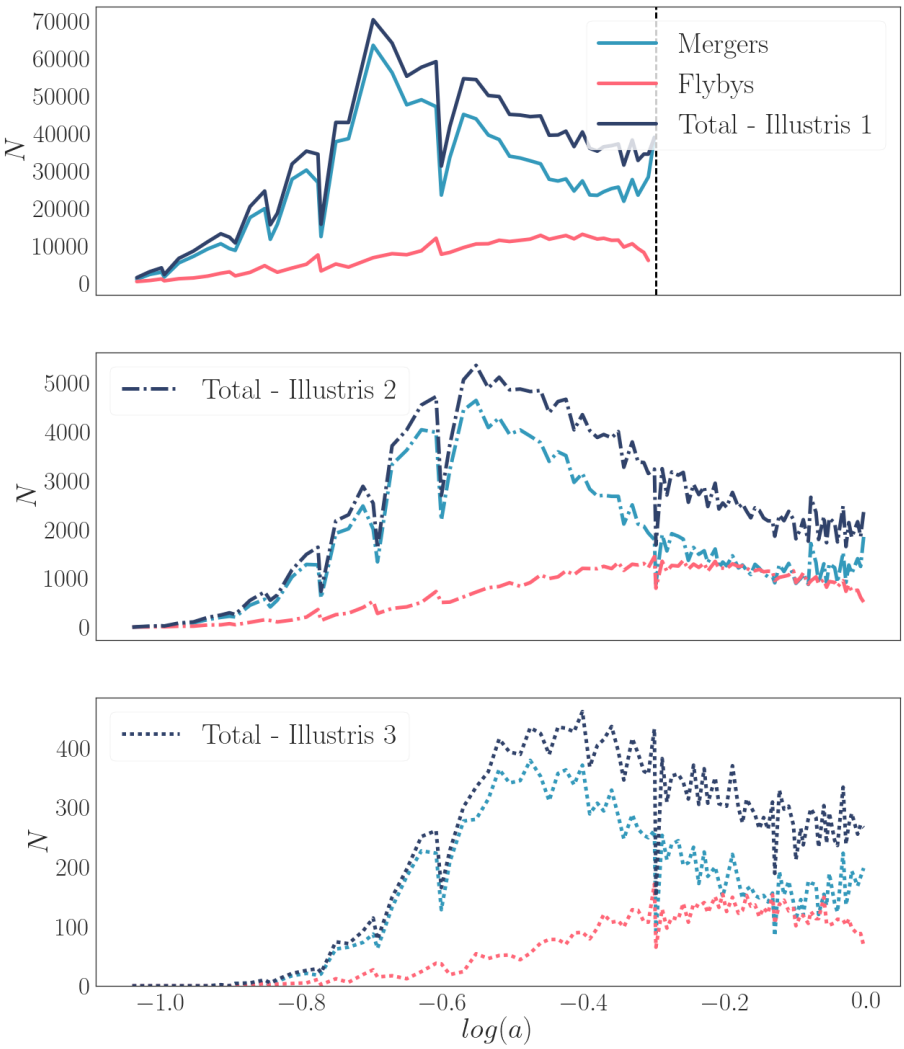

Figure 2.5: Number of mergers, flybys, and total interactions in Illustris-1, Illustris-2, and Illustris-3 hydro at each time in light blue, pink, and navy respectively. The vertical line shows $z = 1$ where data collection ends for the Illustris-1 simulation. As resolution increases the total number of interactions increases dramatically, implying small mass halos are responsible for a large portion of both flybys and mergers.

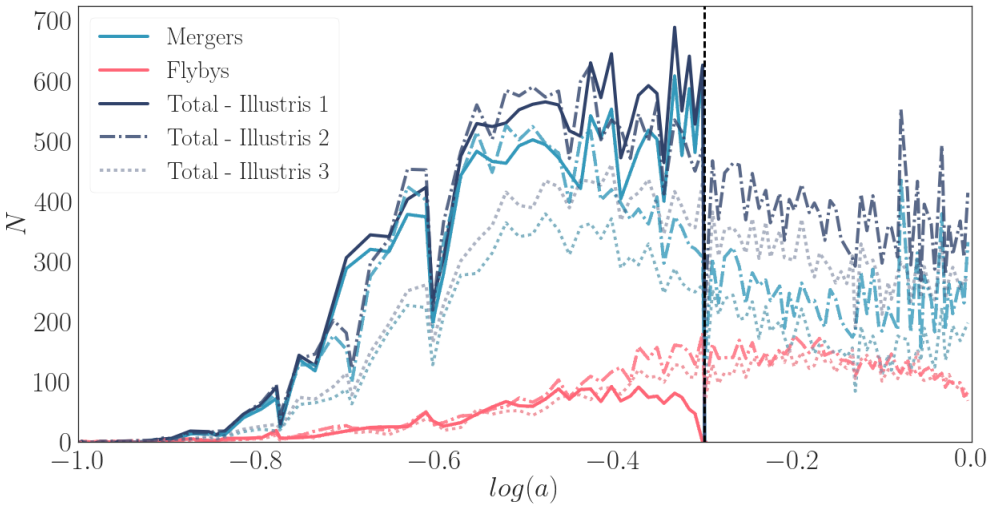

Figure 2.6: Number of mergers, flybys, and total interactions in blue, pink, and navy respectively for each of the hydro runs for all halos with masses above $4 \times 10^{10} M_{\odot}$. Solid lines (dashed, dotted) show data from Illustris-1 (Illustris-2, Illustris-3). The steep decline in flybys at the end time for each run is due to the fact that flybys must be identified by knowing the halo's future outcome, so it is impossible to identify flybys in the last few time steps of a simulation. Ignoring the decline in number of flybys in Illustris-1 prior to end of run, the number of flybys in the mass range of each simulation agrees. There is a slight disparity between Illustris-3 and the higher resolution runs when looking at the number of mergers and thus the number of interactions. This is due to the fact that the plotted mass range is determined by the resolution of Illustris-3, and therefore any halos that drop below that mass limit during a merger will be lost. Overall, the trend of a merger epoch preceding a flyby epoch is evident in each of the Illustris runs.

It is clear that mergers dominate in number across all early times when compared to the number of flybys in each simulation. It can be seen that peak merging activity peaks as early as log(a) = −0.7, or a redshift of $z = 4$ in Illustris-1. It is relevant to consider that mergers are tagged at the moment of halo infall and the duration of a merger can be on the order of Gyrs.

The precise location of the peak from either flybys or mergers is dependant on mass resolution. The peak happens earlier with increasing resolution indicating that the inclusion of small halos that merge early dictates the time frame of peak merger activity. Since mergers dominate the total number of interactions overall, as the merger epoch ends, and

flybys become more common, there is a large drop in the total number of interactions as time goes on. It should be noted that since our definition of flyby requires a minimum of three snapshots, and could take much longer, there will inevitably be a drop in the number of flybys just before the final timestep in any simulation. This could also cause a minor uptick in the number of mergers during the last few timesteps due to the fact that halos that may appear to be merged, but as time goes on it is possible they could escape the potential of their host and be reassigned as a flyby.

Regardless of resolution, each simulation shows an overall larger number of mergers than flybys at early times, which we will call the **merger epoch**, followed by a sharp decrease in merging halos at which time mergers and flybys are approximately equal in number; we will call this the **flyby epoch**. The merger epoch is roughly identified as the time between log(a) = −0.9 to −0.4 (up to z = 1.5), and the flyby epoch spans log(a) = −0.4 to log(a) = 0 (from z = 1.5 to z = 0).

Figure 2.6 applies a uniform mass cut across all three hydrodynamical simulations of $4\times10^{10}M_{\odot}$ corresponding to the smallest resolved halo in the lowest resolution simulation. Illustris-3 tends to under-count the number of mergers relative to Illustris-1 and Illustris-2, likely due to the effects of disappearing halos and incompleteness in the lowest mass bin. Because the flyby fraction is highest for low mass halos, reducing the resolution eliminates a significant number of small halos are likely to interact with halos of resolved mass, and thus lowers the overall flyby and merger counts. However, both Illustris-1 and Illustris-2 agree extremely well in the time before z=1. Despite this minor difference, there is close agreement in relative numbers of flybys and mergers in each iteration of the simulation.

Comparing the simulations in this way confirms the presence of distinct merger and flyby epochs across all 3 runs. With differing mass resolution the initial rise of the merger epoch will vary, but the drop in merging interactions and persistence of flybys at late times remains the same regardless of resolution. It is also significant to note how few interactions happen above this mass cut compared to the total numbers in Illustris-1 and Illustris-2 as

seen in Figure 2.5. It is clear that the overwhelming majority of all counted interactions involves a dwarf-sized halo.

It is well-accepted that interaction rates depend on halo mass, so we explore the rates of flybys and mergers as a function of both log(a) and halo mass. Figure 2.7 bears this out, considering interactions experienced by both the primary and the secondary. We advise to keep in mind that bins at either edge of the mass range will have larger error due to low numbers of halos at high masses and frequent disappearance of halos near the lower mass resolution limit. Mergers per halo at the low mass-end are more rare in the early universe, while the highest mass halos at any time experience about 1000 mergers/halo/Gyr. Flybys are not as numerous in the early universe, however, as log(a) increases flybys become increasingly common. Multiple flybys per halo are most common at the highest masses, but extending down to $\log(M_{halo}) \sim 10^{10}[M_{\odot}/h]$ one could still expect about one flyby per halo per Gyr near the present epoch. This emphasizes the idea that there was a *merger epoch* between $-0.9 < \log(a) < -0.4$, followed by a *flyby epoch* extending from $\log(a) > -0.4$ to today.

To more closely inspect the differences between the number of mergers and number of flybys, we present the ratio of flybys to mergers in each bin of mass and time in Figure 2.8. Near $z = 0$, we find that flybys are as or more numerous than mergers, particularly among low-mass halos. In Illustris-3, between $-0.8 < \log(a) < -0.4$ ($3 < z < 1.5$) mergers are far more numerous across all mass bins. There is a tentative hint that flybys become more common at $\log(a) = -1.0$, though we caution that there is large scatter due to few halos, and this trend ceases upon inspecting the higher resolution runs. We see clearly that there are two distinct areas of interest: 1) the merger dominated era in the early universe in which the most massive halos host the most mergers per halo, and the flyby epoch as we approach today, where low mass halos experience more flybys per halo than mergers, and high mass halos have comparable numbers of both types of interactions. The separation between these two times happens at about $\log(a)=-0.4$ or $z = 1.5$. According to Figure 2.8

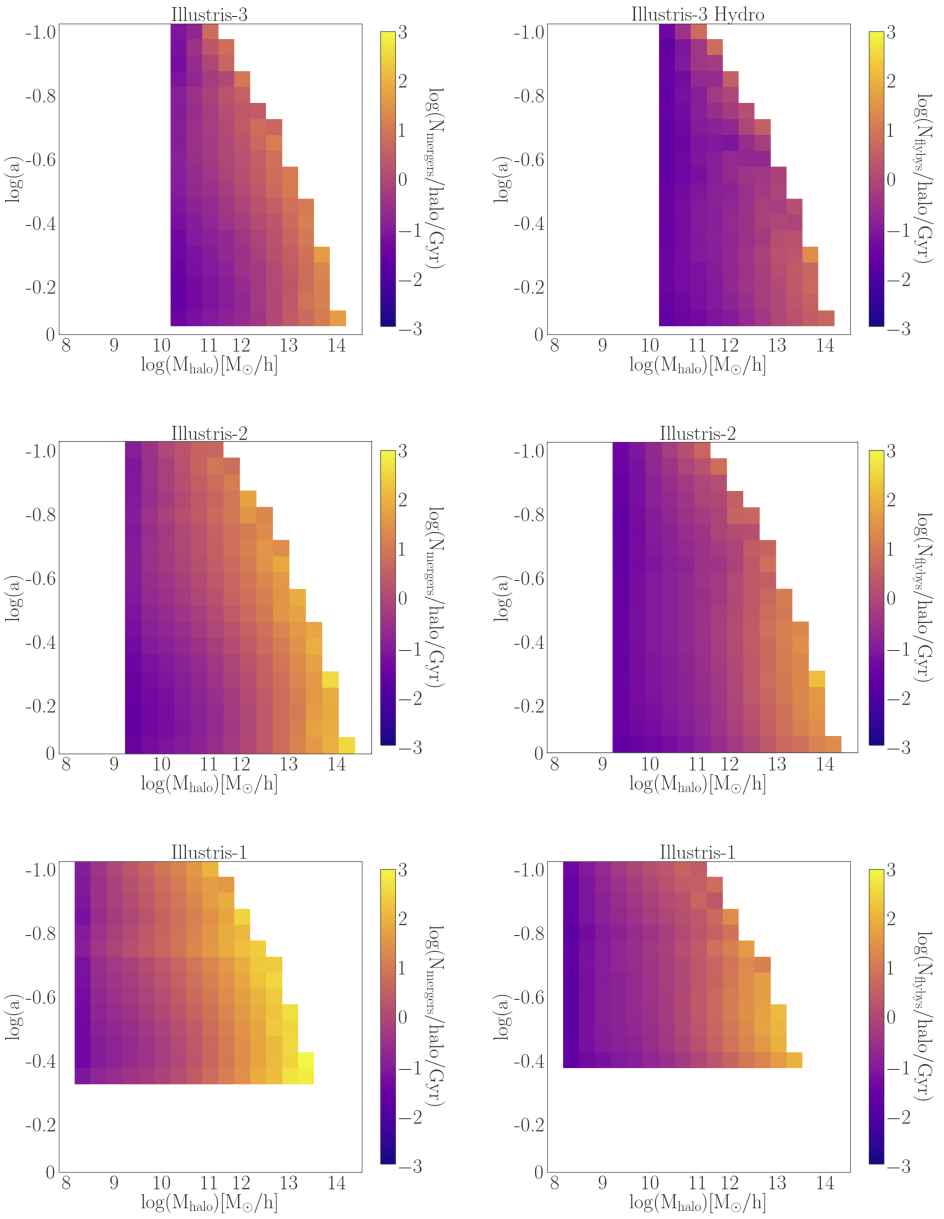

Figure 2.7: Merger rates (left) and flyby rates (right) are shown as a function of both log(a) and primary halo mass. The value in each cell represents the logged number of each type of interaction per halo, per Gyr. The rows from top to bottom, show results from Hydro runs of Illustris-3, Illustris-2, and Illustris-1. The general trend of finding more flybys and mergers per halo at larger masses and smaller $log(a)$, lower z, is consistent across simulations. However, due to the increasing number of halos at the low mass end with higher resolution, the absolute number of flybys and mergers per halo increases with resolution.

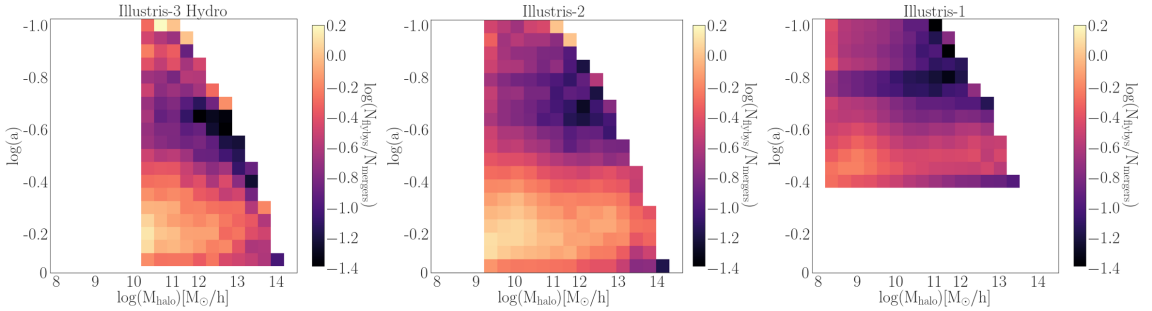

Figure 2.8: The ratio of flybys to mergers as a function of halo mass and time, with the color scale signifying the ratio of flybys to mergers in log scale. From left to right are results from Illustris-1, Illustris-2, and Illustris-3. This more clearly illustrates the separation of merger and flyby epochs. Using data from Illustris-2, a Milky Way mass halo ($\sim 1\times10^{12}M_{\odot}$) at $z=0$ would expect 90% as many flybys as mergers when resolving halos above $4\times10^{9}M_{\odot}$.

a Milky Way mass halo of $10^{12}M_{\odot}$ at $z=0$ is expected to experience flybys and mergers at about the same rate, which we predict to be on the order of 10 per Gyr. For a Virgo-mass halo at 10^{13} the total number of mergers can exceed 100 per Gyr, and would expect about 80% as many flybys as mergers per Gyr.

This could mean that merger rates estimated from simulations, or counting close pairs, that do not separate the two categories of interactions may overestimate the number of mergers by a factor of two at late times. This result broadly agrees with that found by Sinha & Holley-Bockelmann (2011) in which they also found flybys and mergers to become roughly equal in number at low redshifts. Their work used a dark matter only simulation, however, and was run only to $z=1$, beyond which we see the number of flybys stabilize and remain relevant at all masses. Sinha & Holley-Bockelmann (2011) also saw mergers and flybys in similar proportion at log(a) $=-1$ or high z, but acknowledged that Poisson error is very high at this stage in the simulation. When looking at our highest resolution simulation, we see mergers dominating the number of interactions at all halo masses in the early universe.

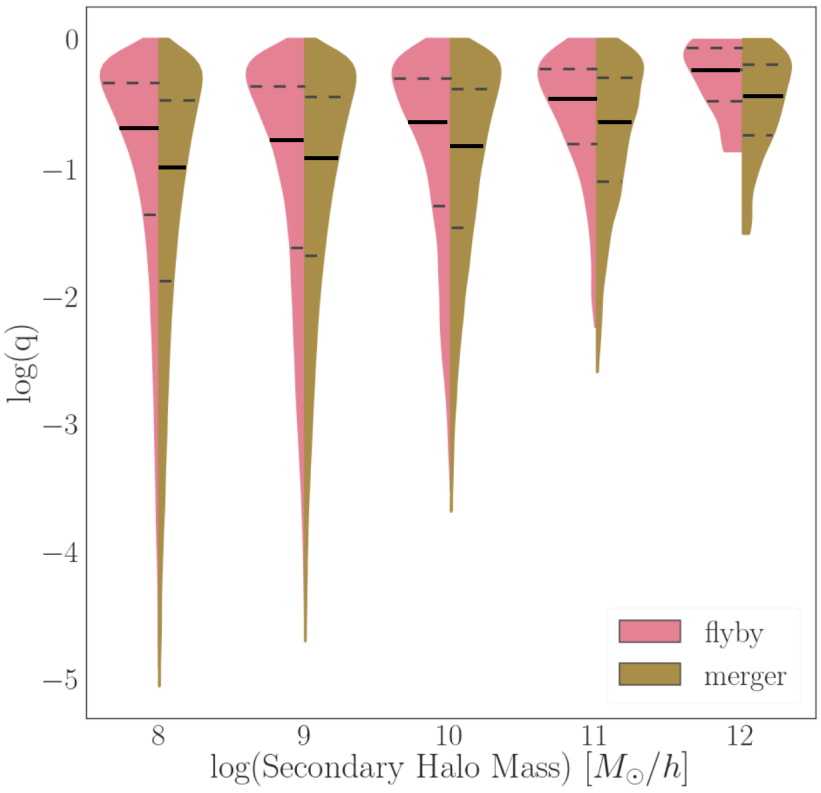

Figure 2.9: Violin plot of the mass ratios as a function of secondary halo mass for mergers (ocher) and flybys (pink). Mass ratio is given as secondary mass/primary mass. The shape of the colored region shows the distribution of the points in each bin. The dotted lines shows the outer quartiles of the distribution. Flybys tend to similar mass ratios while the merging distributions extend to more disparate ones.

2.4.2 Mass Ratio of Interaction

In the previous section, we counted all halos which experienced a flyby as either the victim or the intruder, without considering which halo played each role, or the characteristics of the pair. It is reasonable to think that the halo mass ratio could be a determining factor in whether the interaction will result in a merger or a flyby. We consider the halo which remains a central throughout the interaction the primary, and the halo passing through to be the secondary.

We count each pair and represent the mass ratio in the following way: $q = \frac{M_{\text{secondary}}}{M_{\text{primary}}}$. To look at which masses are involved in each interaction event, we show the pairs of

merging and flyby halos represented by their secondary halo mass, the halo that temporarily becomes a subhalo of the other, in Figure 2.9. The halo masses are binned in $\log(M_{\text{halo,secondary}})$ and the distribution of log(q) are shown for each bin of secondary halo mass.

Because there is a minimum and maximum mass that halos achieved in the simulation, log(q) will have a much larger range of values for small halos who have the opportunity to interact with halos the most different in mass from themselves. This is true for both flybys and mergers. It is also possible, but uncommon, for some pairs to achieve $\log(q) > 0$ in the case that the halos are very similar in mass and the more massive halos is assigned as a subhalo to the less massive during the event.

In any given mass bin, flybys tend to more similar mass ratios, whereas when masses become more disparate, merging becomes a more likely scenario. The difference between the two populations appears most pronounced for the lowest resolvable halos, $10^8 M_\odot$. These are also the halos which are expected to most commonly be the intruders of flyby encounters at low redshifts.

To determine if the distributions of merging and flyby halos in each bin of $\log(M_{\text{halo,secondary}})$ are distinct, we plot the mean of log(q) with errors showing the standard error on the mean for each bin of mass in Figure 2.10. For each mass bin flybys favor more similar masses between the halos when compared to mergers. We find that the difference is most well defined for the lowest halo mass bin of halo mass = $10^8 M_\odot$, but the distributions of flybys and mergers are distinct in each bin of mass, and standard errors are only large enough to plot visibly in the highest mass bin.This is due to the large number of halos in the lower mass bins, and fewer secondary halos with high masses. Using a KS-test confirms that the distribution within each mass bin differs significantly between the merging halos and the flyby halos.

This tells us that the average of either merging or flyby populations are distinct. However, as seen from Figure 2.9 there is significant overlap between the distributions in the

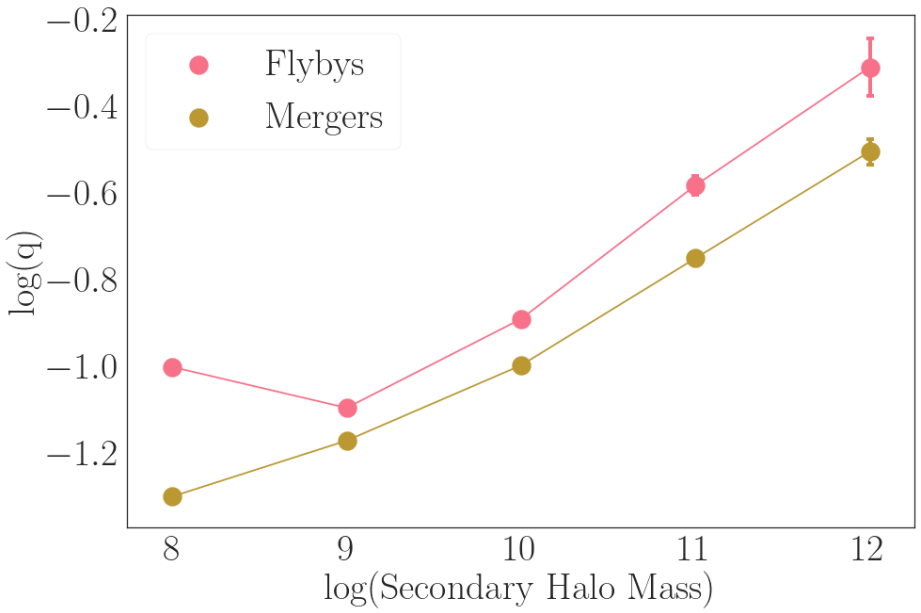

Figure 2.10: Mean of the log(mass ratio) for bins of log(Halo Mass). Errorbars show error on the mean for each point, but are only visibly large in the last bin due to low numbers of secondary halos at that mass.

most common mass ratios between $-1.5 < log(a) < 0$. Therefore knowing only the mass ratio of an interaction for a given secondary halo mass would not be enough to inform you of the outcome of that interaction.

2.4.3 Proximity of Interaction

The impact parameter of the intruding halo's orbit is expected to drive the perturbation on the primary (Sinha & Holley-Bockelmann, 2015). To characterize this, we investigate the ratio of the pericenter distance over $R_{mean,200}$, the comoving radius of a sphere centered on the primary FoF halo whose mean density is 200 times the mean density of the Universe. We choose to use the radius of the FoF halo as it represents all mass of the halo family, including the subhalos associated with that FoF.

Figure 2.11 shows the probability density distributions of key moments in halos' orbits. We show the closest approach for flyby halos in pink, and find that most pericenters are concentrated around $1.5-2R_{\mathrm{mean},200}$ of the host halo. While it may seem like this is outside

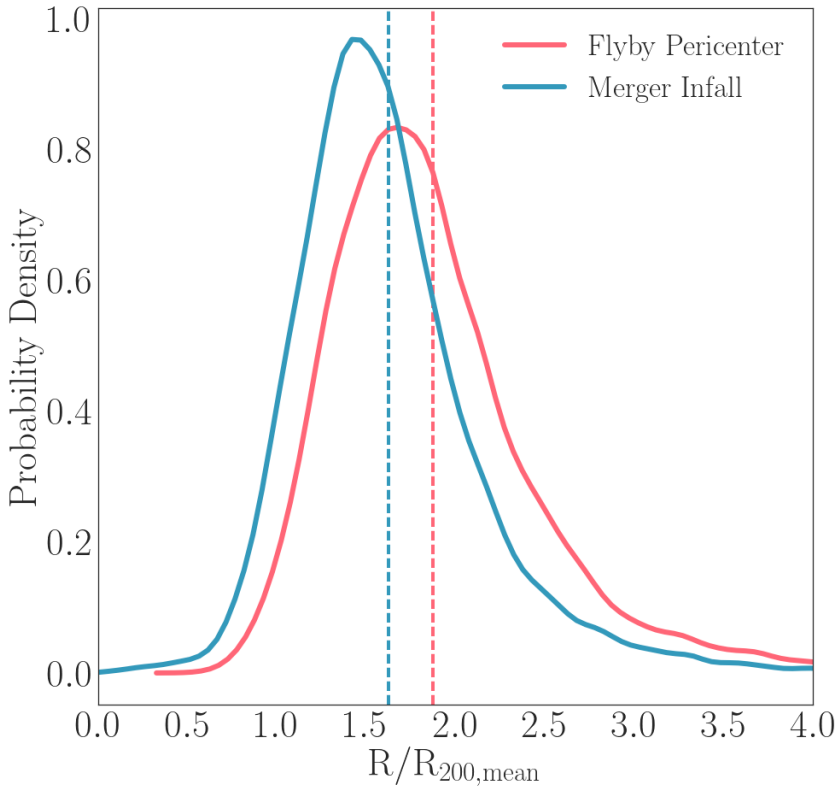

Figure 2.11: Probability density function of flyby orbit pericenters (pink curve) in terms of the primary halo's FOF $R_{200,mean}$ radius. As flybys are generally quick encounters, there is very little time for the intruder to delve deeply inside the $R_{200,mean}$ radius of the host. To compare, we show the distance of merging halos at infall, the first point in time where the the halo is tagged as a subhalo of the other (light blue curve). Averages of each curve are plotted as dashed vertical lines. Mergers experience infall at slightly closer distances to the host.

the halo, it is important to remember that halos are non-spherical (see Figure 2.3). In most scenarios, flybys are extremely short-lived and remain a subhalo for only 1 snapshot ($\sim 500 Myrs$) in which case the orbit skirts the outer edge of the primary halo.

To compare the flybys and mergers, we plot the merger infall distance in light blue as well as the closest detected position of the merged subhalo with its host. Infall is considered to be the first point at which a halo is tagged as a subhalo of the host. We see that even upon infall, flybys tend to happen farther out than mergers. The mean of each distribution is shown with a dashed vertical line in the corresponding color. We find a mean merger infall distance of 1.6 $R/R_{200,mean}$ and a mean flyby pericenter of 1.9. Figure 2.11 also highlights the fact that subhalo capture for both flybys and mergers happens outside of $R_{200,mean}$.

Nevertheless, we see a significant difference between the halos that are able to escape the close encounter as flybys and those that are destined to become trapped inside the host. We note that flybys are plotted here as one distribution regardless of their final outcome (merging flybys and pure flybys) because all categories share the same mean and shape due to their rapid engagement with the host.

2.4.4 Velocity of Interaction

To further map out flyby parameter space, we look at the relative velocities between the two halos involved in the interaction. One might suspect that flybys would enter the encounter with greater relative velocity and thus have enough energy to escape an immediate capture by the host.

Figure 2.12 shows the resultant relative velocities normalized by the escape velocity of the host for both flybys and mergers. While all distributions peak near the escape velocity, flyby events are, on average, happening at higher relative velocities above the escape velocity of the host. The median V_{rel} of mergers happens at $1.1 V_{esc}$, while the median of flybys has a value of $1.4 V_{esc}$.

We found that 50% of flybys will eventually end in merger with the halo they engaged

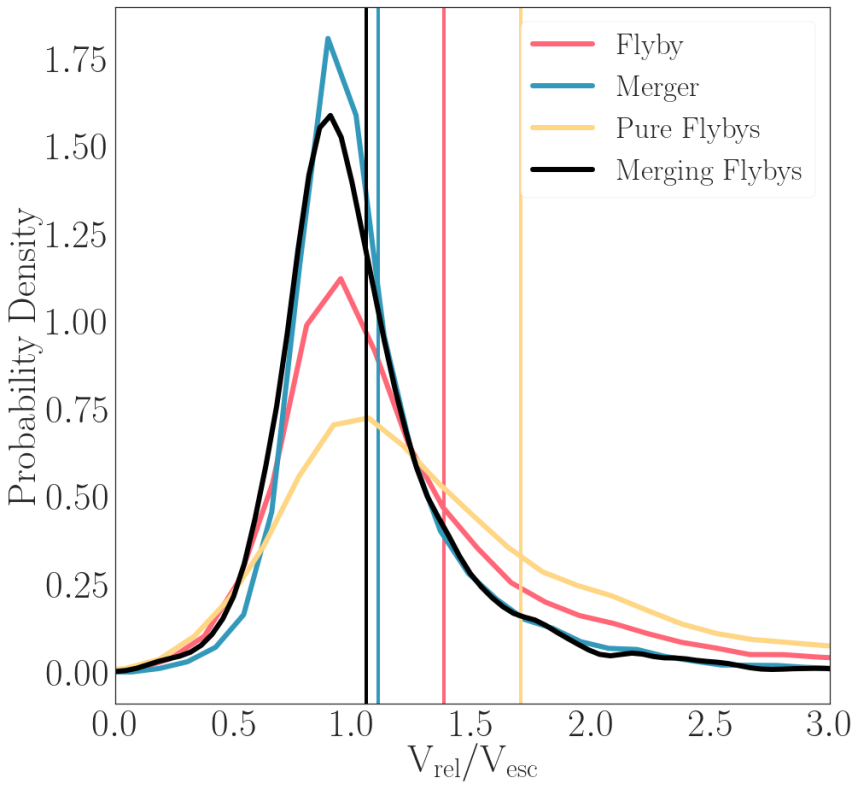

Figure 2.12: Probability density distributions of the relative velocities of flybys and mergers. Velocities are given as the difference in velocity between the primary and the secondary and normalized by the escape velocity of the host halo. Pure Flybys are made up of the flybys that do not end in merger, while merging flybys eventually end in a merger between the halos.

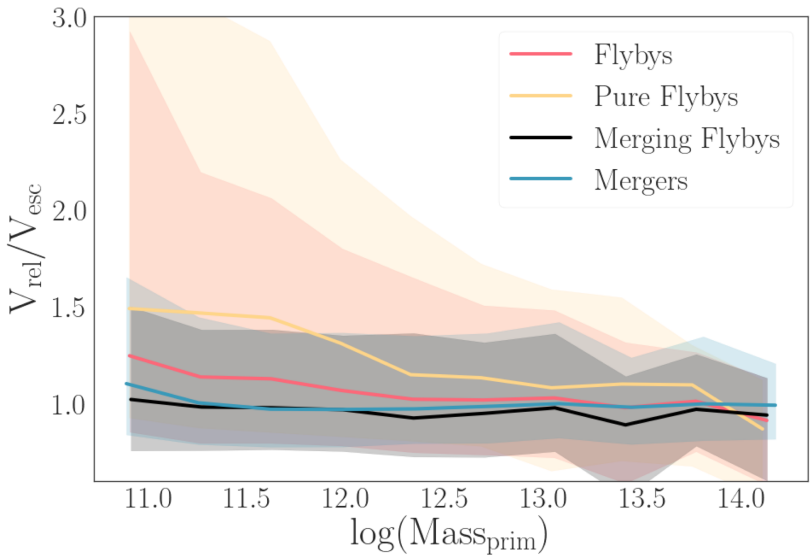

Figure 2.13: Relative velocities between the primary and secondary halo in terms of the escape velocity of the host of flybys and mergers as a function of halo mass of the primary. The average value of the distribution is plotted, and the shaded regions show the 1-sigma confidence interval. Smaller primaries show a greater velocity difference, with pure flybys having the highest V_{rel}.

with, while the other half of halos escape that particular halo's influence until either the end of the simulation or it interacts with another halo. We show the distributions of pure flybys and merging flybys and find that pure flybys have the highest V_{rel} with an average of 1.7 V_{esc}. We also see that in velocity, merging flybys are extremely similar to the merging category. This supports the idea that relative velocity is an important feature when determining not only the immediate fate of a halo pair, but their long-term outcome as a pure flyby or the initial orbits before a merger.

To identify which mass halos of either encounter are subject to these velocity trends we look at V_{rel}/V_{esc} as a function of halo mass for both the primary in Figure 2.13. The difference in relative velocity is most noticeable at small primary masses where the flybys are moving at higher relative velocities compared to both the merging halos and merging flybys. We find that for log(M$_{prim}$) > 12.5 the relative velocities are very similar. Errors are represented by showing where 68% of the data in each bin is contained, however for

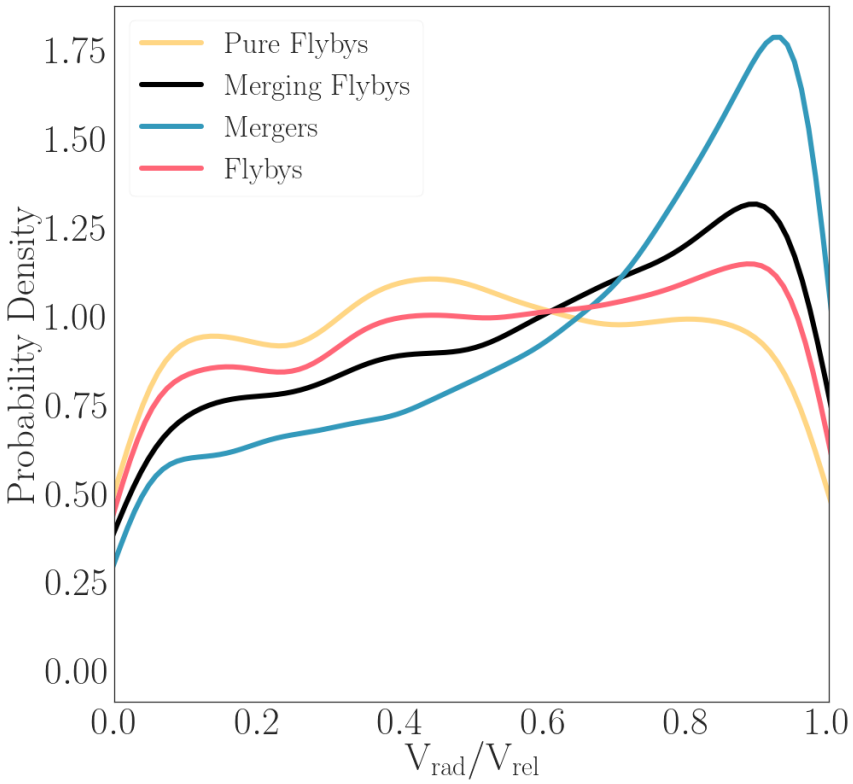

Figure 2.14: Probability density distributions showing the fraction of the relative velocity that is in the direction of the host. Flybys tend to be more grazing encounters than mergers and merging flybys.

both primaries and secondaries, the highest mass bins have very few points.

We have seen that most flyby encounters are grazing rather than radial orbits. Figure 2.14 bears this out: we show probability distributions of ratio of radial and relative velocity. The merging distribution is clearly more radial, as opposed to the pure flybys, which seem to imply a wide span of eccentricities.

2.4.5 Effects of Baryons on Interactions

As the Illustris suite has dark matter only (DMO) runs for each of their simulations to accompany the hydrodynamic runs, we tested the number of flybys and mergers found in Illustris-3 versus those found in Illustris-3 Dark. Other groups have investigated the

differences in subhalo populations with the inclusion of baryons and found mild changes in subhalo shape, infall time, and abundance at low masses (Chua et al., 2019, 2017). Overall, research shows that baryons and their associated feedback processes have a net disruptive effect on lower mass subhalos, as well as changing the density distribution from being peaked to more cored and creating an more expansive stellar halo (Despali & Vegetti, 2017; Zhu et al., 2016; Brooks et al., 2013; Zolotov et al., 2012; Brooks & Zolotov, 2014; El-Badry et al., 2016; Beltz-Mohrmann & Berlind, 2021).

We look at the total numbers of halos across the entire run of the simulation to estimate the overall effect of baryons. We see a net disruptive effect on halos in the hydrodynamic run which results in fewer halos overall at all masses. For a Virgo cluster-sized halo of 10^{13}, we find 25% more instances of a halo of this size in the dark matter iteration across all time. However, errors are large in the high mass bins due to a low number of halos at this mass. These halos take a long time to establish and thus are not nearly as numerous as the dwarf-sized halos. For small halos between $10^{10.5} - 10^{12} M_{\odot}$ there are $10 - 15\%$ fewer halos in the hydro version of Illustris-3.

Figure 2.15 shows the total number of mergers, flybys, and interactions for Illustris-3 and Illustris-3 Hydro across time. Note that the hydro simulation has fewer total halos. When controlling for the number of halos at each snapshot, the relative number of mergers and flybys agrees extremely well. We find that the number of flybys and mergers per halo is left unchanged by adding baryons, implying including hydrodynamic effects does not greatly change merger or flyby rates.

To more closely examine the differences in halo number between the hydro version and the DMO version of Illustris-3, we look at the halo mass function during three time critical slices. We choose $z = 2$, $z = 1$, and $z = 0.02$ as they represent the merger epoch, the flyby epoch, and the universe close to today. Since the number of halos disrupted is mass dependent, we look more closely at the number of each interaction as a function of mass at these key time periods. Figure 2.16 illustrates that the number of interactions

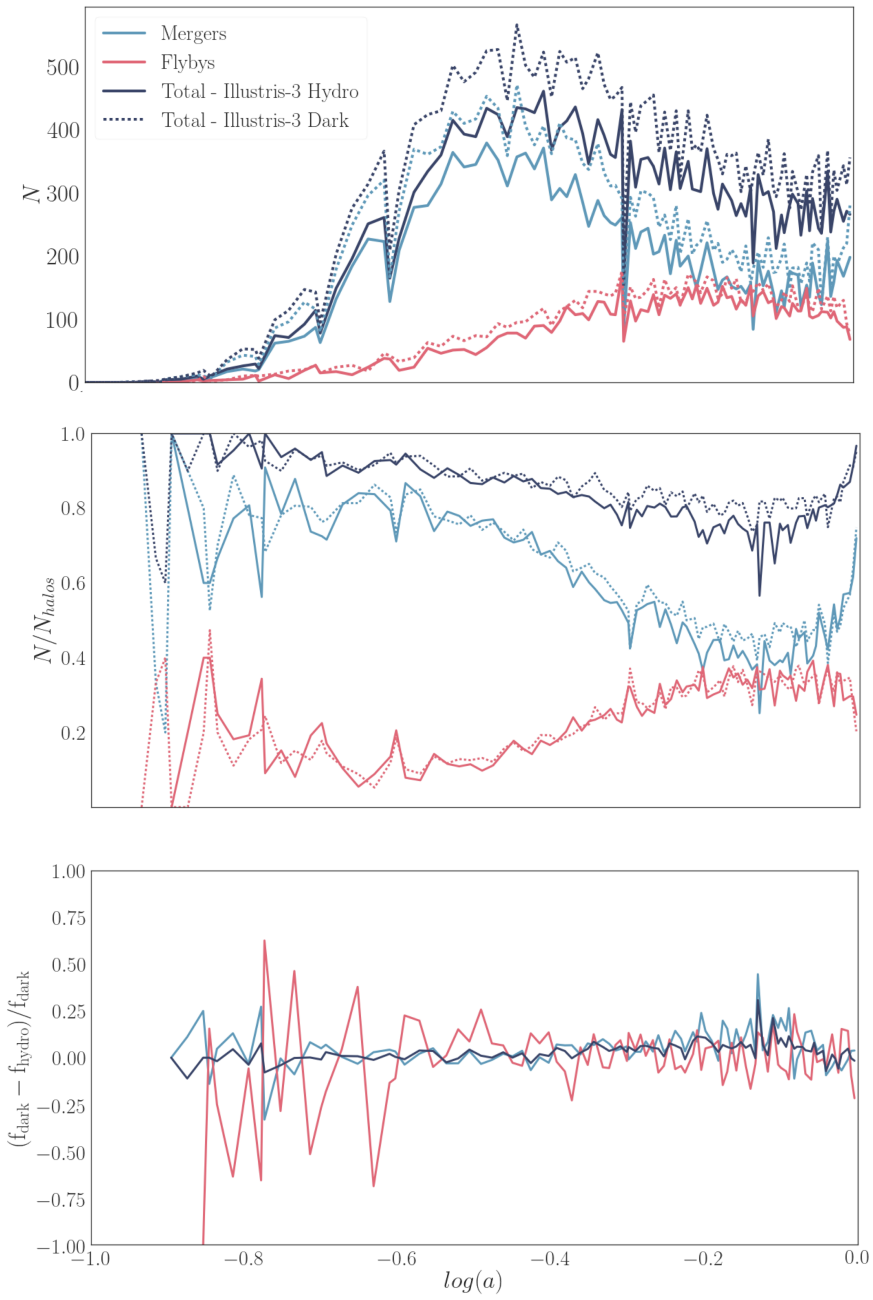

Figure 2.15: Top: The total number of interactions across time for both Illustris-3 Dark and Illustris-3 Hydro with dotted lines and filled lines respectively. Flybys, mergers, and total interactions are shown as in pink, light blue, and navy. Middle: The numbers of each type of interaction normalized by the number of halos present at each time. We find fewer of each type of interaction at all times due to the systematic paucity of halos under the effects of baryons, but very good agreement in the amount of interactions when normalizing by the total number of halos. Bottom: We show residual of N/N_{halos} for dark and hydro as f_{dark} and f_{hydro} respectively for each type of interaction. There does not appear to be any time where the dark and hydro are systematically larger for any time of interaction. Large errors in the flyby counts at low $log(a)$ are due to the low number of flybys.

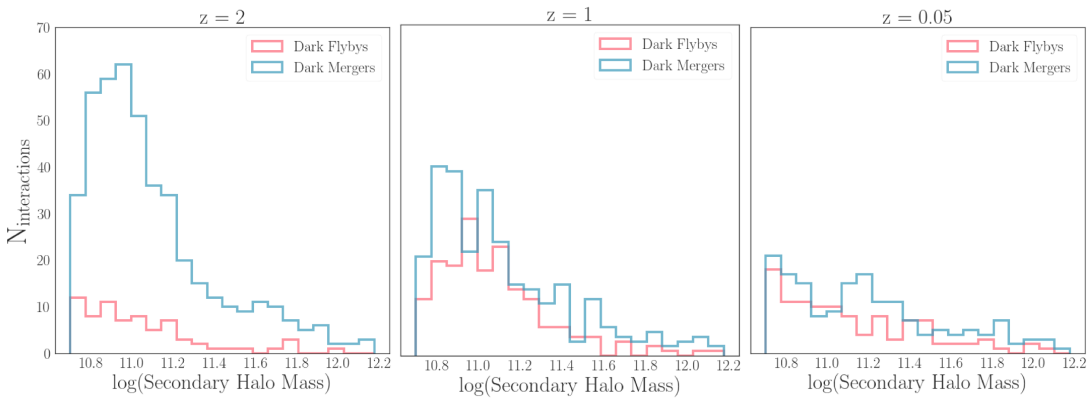

Figure 2.16: The number of mergers and flybys happening at (from left to right) $z = 2$, $z = 1$, and $z = 0.05$ in Illustris-3 Dark. We find distinguishable flyby and merger epochs in the Dark version of Illustris-3. Halo masses for intruders in flyby and merger encounters are similar to those found in Illustris-3 Hydro.

happening at these times remains in close agreement. There is significant prevalence of mergers over flybys at $z = 2$ during the merger epoch, followed by an increase of flybys at $z = 1$ paired with a drop in mergers. At $z = 0.05$ we find fewer of both types of interaction. Even with slight variance in total number of halos, the dependence on mass of each type of interaction is unchanged by the addition of baryonic physics, and the merger and flyby epoch are temporally aligned in both simulations.

The final parameter comparison between the dark and hydro runs concerns the size of the halos. Some studies have seen that the halo sizes can be changed due to baryonic physics. Since gas and stars are subject to feedback, by moving mass outwards the potential well of the halo is altered which could increase the overall size of the parent halo, particularly for small halo masses (El-Badry et al., 2016; Brooks et al., 2013).

We examine the pericenter distance for both versions of Illustris-3 and find the inclusion of baryons does not appear to affect the proximity of an intruder for any primary mass halo. While the hydro secondaries are marginally larger than the dark secondaries, this is an extremely minor trend and does not affect the measured proximity of the interaction. This further confirms that depth of penetration and halo size are negligibly changed for flyby participants.

Overall, the addition of baryons and their feedback processes does not change our primary results on the differences between flybys and mergers. Aside from there being fewer halos in total, flyby and merger rates, masses, and sizes are statistically unaffected by their inclusion. This is expected since flybys as we describe them are dark matter halo encounters which happen on fringes of halos. Baryons are generally found at the centers of dark matter halos where the potential is high and their effects would go unnoticed to the outside edges of a halo of substantive mass.

2.5 Conclusion

We constructed a full halo interaction network for all halos with over 100 particles in several realizations of the Illustris Simulation. The halo interaction network includes all mergers and flybys of any resolved halo throughout the duration of the simulation. Catalogs of these interaction networks are released and available online for all three versions of the hydrodynamic runs of Illustris as well as for Illustris-3 Dark.

We find that as the universe grows it goes through a merger epoch between $-0.9 < log(a) < -0.4$ ($z = 3$ to $z = 1.5$) followed by a flyby epoch that extends from $log(a) = -0.4$ to the present ($z = 1.5$ to $z = 0$). While mergers are greater in number than flybys at most times, during the flyby epoch they occur at approximately equal rates. Both mergers and flybys see an increasing rate per halo as halo mass grows that persists across time. Flybys rival mergers in number during the flyby epoch, where smaller halos see a larger fraction of their interactions being flybys. For a Milky Way mass primary halo at $z = 0$ we predict 90% as many flybys as mergers for secondary halos above $4 \times 10^9 M_\odot$.

Looking closely at the pairs of halos that are interacting, there is some difference between the mass ratios of flybys and mergers, with flybys slightly preferring pairs which are closer in mass. Mergers dominate for pairs with extremely disparate masses, or small values of log(q). Overall, we see a flyby halos interacting with halos more similar in mass to themselves at all secondary masses, however there is significant overlap in these dis-

tributions. It would therefore not be possible to determine the outcome of any individual interaction based only on mass ratio of the halos. For secondary halos of mass $10^8 M_\odot$, the average flyby has a log(q) = −1.0, while the average merger expects a $log(q) = -1.3$. In the case of more massive secondaries, near $10^{12} M_\odot$, mass ratios are much more similar due to the fact that the possible separation between this mass halo and the largest halos is smaller. Mergers at this mass range have an average log(q) = −0.6 and flybys again show more similar masses with average log(q) = −0.3.

We see that most flybys are skirting encounters that generally take place outside the host halo's radius, independent of which spherical overdensity radius one chooses to represent the host. Since our definition of flyby relies on whether a halo is considered to be a FoF or a subhalo, it can be sensitive to the halo finder used, but this also allows us to substructure bound to asymmetric halos. We find that most halos are not well-represented with a spherical boundary and can host subhalos in long extending arms which protrude out to a few $R_{200,mean}$.

Most flybys do not dive through the center of a larger halo and separate from its host forever. Instead, they are transient and skirting interactions. Most flybys are only subhalos for 500 Myrs, which matches our snapshot resolution at most times. However, this is still half a dynamical time for halos near the virial radius. A typical the flyby pericenter is 1.9 $R/R_{200,mean}$. This emphasizes that flybys are generally able to escape the gravitational hold of their host simply through their wide interaction. Higher temporal resolution would further illuminate the true duration and pericenter of the encounter.

Although the peak of the infall velocity distribution in flybys is the same as in that of mergers, there is a significant high velocity tail for flybys; the pure flyby velocity distribution average is 1.7 V_{esc}, whereas mergers yield $1.12 V_{esc}$. By isolating the 50% of flybys that do not end in merger with same host, pure flybys, we find they have the highest relative velocities of all categories with an average of 1.7 V_{rel}. We also discovered that mergers and merging flyby favor a more radial relative velocity, while flybys tend to have more of their

population in grazing encounters.

We built the halo interaction network for three realizations of the hydrodynamic Illustris Simulation which allowed us to gauge the effect that resolution has on our flyby study. We confirm the two distinct epochs of interactions, with mergers occurring much earlier than flybys for all resolutions. We characterize the generic merger epoch as the time between z=3 to z=1.5, and the flyby epoch as the time from z=1.5 to z=0. However, with the inclusion of lower mass halos, flyby and merger rates increase dramatically as these small halos make up a large percentage of the total flybys and mergers. As small halos form earlier in the simulation, probing smaller masses causes the initial increase in merger activity to shift to earlier times. For Illustris-1 (which resolves halos above $4.4 \times 10^8 M_\odot$) peak merger activity happens as early as $log(a) = -0.7$ whereas in Illustris-3 (resolving halos above 4.4×10^{10}) peak merger activity occurs at $log(a) = -0.5$.

An interaction network for Illustris-3 Dark was also constructed to investigate any differences induced by running the simulation with baryons. As other groups have noted, we find fewer halos at all masses in the hydrodynamic run of Illustris-3. After normalizing for the total number of halos found in the simulation, we see fantastic agreement in the rates of mergers and flybys at all times and across all mass ranges. We find similar skirting behavior of flybys, and negligible differences in the sizes of the parent halos between the two simulations. We conclude that there are no major differences in rates, epoch time, or pericenter passage seen in hydrodynamic simulations versus dark matter only simulations.

All interaction networks for the simulations are publicly available online at https://doi.org/10.5281/zenodo.5136803. We think this could be useful in studies of measuring baryonic changes induced by flybys. Disentangling the observational signatures of mergers and flybys could provide an opportunity to further understand a galaxy's past. Measuring effects of black hole activity, changes in mass-to-light ratio caused by stripping, or star formation activity are areas of galaxy evolution that could be impacted by flyby encounters.

Acknowledgments

We acknowledge the Vanderbilt Advanced Computing Center for Research and Education (ACCRE). This work used XSEDE resources including the Bridges-2 supercomputer at Pittsburgh Supercomputing Center. This research made use of python (https://www.python.org/), the ipython package (Perez and Granger2007), scipy (Jones et al. 2001), numpy (Van Der Walt et al. 2011), and matplotlib, a Python library for publication quality graphics (Hunter 2007)

Chapter 3

CONCLUSIONS

In this dissertation, we present a complete census of all flybys and mergers in several iterations of the Illustris Simulation. For Illustris-3, Illustris-3 Dark, Illustris-2, and Illustris-1 (to $z = 1$) we compute merger and flyby rates and characterize what properties lend themselves to resulting in either type of interaction. We share these interactions publicly on https://doi.org/10.5281/zenodo.5136803. Flybys have previously been overlooked as a relevant driver of galaxy evolution, but we find from hydrodynamic cosmological simulations that their rates rival that of mergers at the present epoch.

Our results broadly agree with what was found in dark matter only simulations in Sinha & Holley-Bockelmann (2015). We find that regardless of resolution or baryonic inclusion, the time period from z=1.5 to z=0 contains as many flyby interactions as mergers for many halo masses. Small halos are more likely to be the intruder in a flyby encounter with a flyby fraction of about 1% for $10^9 M_\odot$ halos. We also find that flybys tend to more similar mass ratios while mergers dominate the highly disparate mass ratio encounters between halos. Flybys that do not ever end in merger tend to happen at higher velocities compared to mergers and mergers have more of their velocity in the radial direction of the host.

Overall, we find flybys to mostly be rapid and grazing encounters in the outskirts of a halo. However, it has been shown that interactions outside of the main halo are able to incite resonant interactions that have the potential to alter the galaxies within. Lang et al. (2014) has shown that flybys in high mass ratio interactions are able to incite bars or completely destroy the secondary in the interaction. Wetzel et al. (2014) has shown also shown that including flybys in the cosmological perspective could explain populations of quenched, red galaxies living outside of clusters in the splashback region of larger hosts.

We have shown that large halos with masses comparable to the Virgo cluster $\sim 10^{13} M_\odot$,

one can expect as many as 100 mergers per Gyr, and about 80 flybys per Gyr. This warrants further investigation into the after effects of flybys on the intruder and host galaxies. The effects of flybys have been hypothesized to be similar to that of a minor merger (Vesperini & Weinberg, 2000) which could have observational signatures such as induced star formation, bars, AGN, or changes in color, or mass-to-light ratio. Since our interaction catalog references all baryonic properties from the Illustris simulation database, we believe this presents an opportunity to further study the observational signatures of flybys in the universe.

REFERENCES

Ade P. A. R., Aghanim N., Arnaud M., et al., 2016, Astronomy Astrophysics, 594, A13

Adhikari S., Dalal N., Chamberlain R. T., 2014, , 2014, 11, 019

Angulo R. E., Lacey C. G., Baugh C. M., Frenk C. S., 2009, , 399, 983

Athanassoula E., Rodionov S. A., Peschken N., Lambert J. C., 2016, , 821, 90

Balogh M. L., Navarro J. F., Morris S. L., 2000, , 540, 1, 113

Barnes J. E., 1988, , 331, 699

Barnes J. E., 2002, , 333, 481

Barnes J. E., Hernquist L., 1992, , 360, 6406, 715

Barton Gillespie E., Geller M. J., Kenyon S. J., 2003, , 582, 668

Bekki K., Couch W. J., 2011, , 415, 2, 1783

Beltz-Mohrmann G. D., Berlind A. A., 2021, The impact of baryonic physics on the abundance, clustering, and concentration of halos

Berlind A. A., Weinberg D. H., Benson A. J., et al., 2003, , 593, 1, 1

Bertschinger E., 1985, , 58, 39

Bertschinger E., 1998, , 36, 599

Boylan-Kolchin M., Springel V., White S. D. M., Jenkins A., Lemson G., 2009, , 398, 1150

Brooks A. M., Kuhlen M., Zolotov A., Hooper D., 2013, The Astrophysical Journal, 765, 1, 22

Brooks A. M., Zolotov A., 2014, The Astrophysical Journal, 786, 2, 87

Buck T., Macciò A. V., Dutton A. A., Obreja A., Frings J., 2019, , 483, 1, 1314

Bushouse H. A., 1987, , 320, 49

Calura F., Menci N., 2011, , 413, 1, L1

Chua K. T. E., Pillepich A., Rodriguez-Gomez V., Vogelsberger M., Bird S., Hernquist L., 2017, Monthly Notices of the Royal Astronomical Society, 472, 4, 4343–4360

Chua K. T. E., Pillepich A., Vogelsberger M., Hernquist L., 2019, Monthly Notices of the Royal Astronomical Society, 484, 1, 476–493

Clauwens B., Schaye J., Franx M., Bower R. G., 2018, , 478, 3994

Cox T. J., Jonsson P., Primack J. R., Somerville R. S., 2006, , 373, 1013

Dahari O., 1984, , 89, 966

Davis M., Efstathiou G., Frenk C. S., White S. D. M., 1985, , 292, 371

Despali G., Vegetti S., 2017, Monthly Notices of the Royal Astronomical Society, 469, 2, 1997–2010

Di Matteo T., Springel V., Hernquist L., 2005, in Growing Black Holes: Accretion in a Cosmological Context, edited by A. Merloni, S. Nayakshin, R. A. Sunyaev, 340–345

Diemer B., 2018, , 239, 2, 35

Diemer B., 2021, , 909, 2, 112

D'Onghia E., Vogelsberger M., Faucher-Giguere C.-A., Hernquist L., 2010, , 725, 1, 353

Dubinski J., 1999, in Galaxy Dynamics - A Rutgers Symposium, edited by D. R. Merritt, M. Valluri, J. A. Sellwood, vol. 182 of Astronomical Society of the Pacific Conference Series

Dubinski J., Chakrabarty D., 2009, , 703, 2, 2068

Einasto J., Kaasik A., Saar E., 1974, Tartu Astrofüüs. Obs. Preprint, Nr. 1, 8 p., 1

El-Badry K., Wetzel A., Geha M., et al., 2016, , 820, 2, 131

Fillmore J. A., Goldreich P., 1984, , 281, 1

Gao L., Springel V., White S. D. M., 2005, , 363, 1, L66

Genel S., Genzel R., Bouché N., et al., 2008, , 688, 789

Genel S., Genzel R., Bouché N., Naab T., Sternberg A., 2009, , 701, 2002

Genel S., Vogelsberger M., Springel V., et al., 2014, Monthly Notices of the Royal Astronomical Society, 445, 1, 175–200

Genel S., Vogelsberger M., Springel V., et al., 2014, , 445, 175

Gottlöber S., Klypin A., Kravtsov A. V., 2001, , 546, 223

Guo Q., White S. D. M., 2008, , 384, 2

Haggar R., Gray M. E., Pearce F. R., et al., 2020a, , 492, 4, 6074

Haggar R., Gray M. E., Pearce F. R., et al., 2020b, arXiv e-prints, arXiv:2001.11518

Heckman T. M., Smith E. P., Baum S. A., et al., 1986, , 311, 526

Hernquist L., Mihos J. C., 1995, , 448, 41

Hernquist L., Weinberg M. D., 1989, , 238, 407

Hinshaw G., Larson D., Komatsu E., et al., 2012

Holley-Bockelmann K., Richstone D. O., 2000, , 531, 232

Holley-Bockelmann K., Weinberg M., Katz N., 2005, , 363, 991

Holmberg E., 1941, , 94, 385

Hopkins P. F., Bundy K., Croton D., et al., 2010a, , 715, 202

Hopkins P. F., Hernquist L., Cox T. J., et al., 2005, , 630, 705

Hopkins P. F., Hernquist L., Cox T. J., Di Matteo T., Robertson B., Springel V., 2006, , 163, 1

Hopkins P. F., Kereš D., Ma C.-P., Quataert E., 2010b, , 401, 1131

Hopkins P. F., Quataert E., 2010, , 407, 3, 1529

Hu J., 2008, Monthly Notices of the Royal Astronomical Society, 386, 4, 2242–2252

Joseph R. D., Meikle W. P. S., Robertson N. A., Wright G. S., 1984, , 209, 111

Kennicutt Jr. R. C., Keel W. C., van der Hulst J. M., Hummel E., Roettiger K. A., 1987, , 93, 1011

Kereš D., Katz N., Fardal M., Davé R., Weinberg D. H., 2009, , 395, 160

Knebe A., Gámez-Marín M., Pearce F. R., et al., 2020, , 495, 3, 3002

Kormendy J., Kennicutt R. C., 2004, Annual Review of Astronomy and Astrophysics, 42, 1, 603–683

Kormendy J., Sanders D. B., 1992, , 390, L53

Lacey C., Cole S., 1993, , 262, 3, 627

Lacey C., Cole S., 1994, , 271, 676

Lambas D. G., Tissera P. B., Alonso M. S., Coldwell G., 2003, , 346, 1189

Lang M., Holley-Bockelmann K., Sinha M., 2014

Larson R. B., Tinsley B. M., 1978, , 219, 46

Laurikainen E., Salo H., Buta R., Knapen J. H., 2007, Monthly Notices of the Royal Astronomical Society, 381, 1, 401–417

Licquia T. C., Newman J. A., 2015, The Astrophysical Journal, 806, 1, 96

Lithwick Y., Dalal N., 2011, , 734, 2, 100

Łokas E. L., 2018, , 857, 6

Ludlow A. D., Navarro J. F., Springel V., Jenkins A., Frenk C. S., Helmi A., 2009, , 692, 931

Lynds R., Toomre A., 1976, , 209, 382

Mahajan S., Mamon G. A., Raychaudhury S., 2011

Mamon G. A., Sanchis T., Salvador-Solé E., Solanes J. M., 2004, , 414, 445

Mansfield P., Kravtsov A., Diemer B., 2017, Phil-Mansfield/Shellfish: Aas Release

Marconi A., Hunt L. K., 2003, , 589, 1, L21

Martín-Navarro I., Brodie J. P., Romanowsky A. J., Ruiz-Lara T., van de Ven G., 2018, Nature, 553, 7688, 307–309

Micic M., Holley-Bockelmann K., Sigurdsson S., 2011, , 414, 1127

Micic M., Holley-Bockelmann K., Sigurdsson S., Abel T., 2007, , 380, 1533

Mihos J. C., Hernquist L., 1996, , 464, 641

Moore B., Katz N., Lake G., Dressler A., Oemler A., 1996, , 379, 613

More S., Diemer B., Kravtsov A. V., 2015, , 810, 1, 36

More S., Miyatake H., Takada M., et al., 2016, , 825, 1, 39

Moreno J., Torrey P., Ellison S. L., et al., 2015, , 448, 1107

Muldrew S. I., Pearce F. R., Power C., 2011, , 410, 2617

Naab T., Burkert A., 2003, , 597, 893

Nelson D., Pillepich A., Genel S., et al., 2015

Nikolic B., Cullen H., Alexander P., 2004, , 355, 874

Ostriker J. P., Peebles P. J. E., 1973, , 186, 467

Penzias A. A., Wilson R. W., 1965, , 142, 419

Peschken N., Łokas E. L., 2018, ArXiv e-prints

Pettitt A. R., Wadsley J. W., 2018, , 474, 5645

Pillepich A., Springel V., Nelson D., et al., 2017

Pimbblet K. A., 2010

Pimbblet K. A., 2011, , 411, 4, 2637

Press W. H., Schechter P., 1974, , 187, 425

Rodriguez-Gomez V., Genel S., Vogelsberger M., et al., 2015, Monthly Notices of the Royal Astronomical Society, 449, 1, 49–64

Rubin V. C., Ford W. K. J., Thonnard N., 1980, , 238, 471

Rubin V. C., Ford W. Kent J., 1970, , 159, 379

Sachs R. K., Wolfe A. M., 1967, , 147, 73

Schweizer F., 1986, Science, 231, 227

Shi X., 2016, , 459, 4, 3711

Shlosman I., Frank J., Begelman M. C., 1989, , 338, 6210, 45

Sinha M., Holley-Bockelmann K., 2011

Sinha M., Holley-Bockelmann K., 2015, arXiv e-prints, arXiv:1505.07910

Sinha M., Holley-Bockelmann K., 2015, A First Look at Galaxy Flyby Interactions. II. Do Flybys matter?

Snyder G. F., Torrey P., Lotz J. M., et al., 2015, , 454, 1886

Springel V., Di Matteo T., Hernquist L., 2005, , 620, L79

Springel V., White S. D. M., 1999, , 307, 1, 162

Springel V., White S. D. M., Tormen G., Kauffmann G., 2001, , 328, 726

Stewart K. R., Bullock J. S., Barton E. J., Wechsler R. H., 2009, , 702, 1005

Toomre A., 1964, , 139, 1217

Toomre A., 1977, in Evolution of Galaxies and Stellar Populations, edited by B. M. Tinsley, R. B. G. Larson, D. Campbell, 401

Toomre A., Toomre J., 1972, , 178, 623

Torrey P., Vogelsberger M., Genel S., Sijacki D., Springel V., Hernquist L., 2013

Tremaine S., Gebhardt K., Bender R., et al., 2002, , 574, 2, 740

Tutukov A. V., Fedorova A. V., 2006, Astronomy Reports, 50, 785

van den Bosch F. C., Ogiya G., Hahn O., Burkert A., 2017, Monthly Notices of the Royal Astronomical Society, 474, 3, 3043–3066

van der Hulst J. M., 1979, , 71, 131

Vesperini E., Weinberg M. D., 2000, , 534, 598

Vogelsberger M., Genel S., Sijacki D., Torrey P., Springel V., Hernquist L., 2013

Vogelsberger M., Genel S., Springel V., et al., 2014, , 444, 1518

Vogelsberger M., Genel S., Springel V., et al., 2014, Nature, 509, 7499, 177–182

Vogelsberger M., White S. D. M., 2011, , 413, 2, 1419

Wechsler R. H., Bullock J. S., Primack J. R., Kravtsov A. V., Dekel A., 2002, The Astrophysical Journal, 568, 1, 52–70

Wechsler R. H., Zentner A. R., Bullock J. S., Kravtsov A. V., Allgood B., 2006, , 652, 1, 71

Weigel A. K., Schawinski K., Treister E., Trakhtenbrot B., Sanders D. B., 2018, , 476, 2308

Weinberg M. D., 1998, , 299, 499

Weinberg M. D., Katz N., 2002, , 580, 2, 627

Weinberger R., Springel V., Hernquist L., et al., 2016

Wetzel A. R., Tinker J. L., Conroy C., Bosch F. C. v. d., 2014, Monthly Notices of the Royal Astronomical Society, 439, 3, 2687–2700

Wetzel A. R., Tinker J. L., Conroy C., van den Bosch F. C., 2013

Wetzel A. R., Tinker J. L., Conroy C., van den Bosch F. C., 2014, , 439, 3, 2687

Whitaker K. E., Rigby J. R., Brammer G. B., et al., 2014, , 790, 2, 143

White S. D. M., 1978, , 184, 185

White S. D. M., 1979, , 189, 831

Wild V., Rosales-Ortega F., Falcón-Barroso J., et al., 2014, , 567, A132

Younger J. D., Hopkins P. F., Cox T. J., Hernquist L., 2008, , 686, 815

Zhu Q., Marinacci F., Maji M., Li Y., Springel V., Hernquist L., 2016, Monthly Notices of the Royal Astronomical Society, 458, 2, 1559–1580

Zolotov A., Brooks A. M., Willman B., et al., 2012, The Astrophysical Journal, 761, 1, 71

Zwicky F., 1937, , 86, 217

Zwicky F., 1956, Ergebnisse der exakten Naturwissenschaften, 29, 344

Zwicky F., 1959, Handbuch der Physik, 53, 373